# Comparison with Different Bayesian and Non-Bayesian Estimation Techniques for the Compound Rayleigh Exponential Distribution with Actuarial Measures and Applications

Ibrahim Hassan Alkhairy and Hassan Alsuhabi*

Department of Mathematics, Al-Qunfudah University College, Umm Al-Qura University, Mecca, 24382, Saudi Arabia


**INFORMATION**

**Keywords:**
Applied sciences
Bayesian estimation
insurance
loss functions
maximum product spacing
Monte Carlo simulation

**DOI:** 10.23967/j.rimni.2025.10.73596

SCIPEDIA Revista Internacional de Métodos Numéricos para Cálculo y Diseño en Ingeniería

Revista Internacional Métodos numéricos para cálculo y diseño en ingeniería RIMNI

In cooperation with CIMNE

# Comparison with Different Bayesian and Non-Bayesian Estimation Techniques for the Compound Rayleigh Exponential Distribution with Actuarial Measures and Applications

**Ibrahim Hassan Alkhairy and Hassan Alsuhabi***

Department of Mathematics, Al-Qunfudah University College, Umm Al-Qura University, Mecca, 24382, Saudi Arabia

**ABSTRACT**

Many lifetime analyses such as those in engineering, biology, survival studies, actuarial, and medical sciences rely heavily on the two-parameter Compound Rayleigh Exponential Distribution (CRED), which is well-established in statistical theory. Due to their effectiveness in handling small sample sizes and incorporating prior knowledge, Bayesian techniques are essential for estimating the parameters of the CRED. This study presents the estimation of the compound Rayleigh exponential distribution unknown parameters using Bayesian and non-Bayesian estimation techniques, including maximum likelihood estimation, maximum product spacing, least square estimator, weighted least square estimator, Cramer-Von-Mise estimator, Anderson-Darling estimator, and Bayesian techniques with informative and non-informative priors based on different loss functions. Additionally, we used several methods to construct confidence intervals for the unknown parameters, including the approximate and bootstrap approaches. The effectiveness of these estimators is evaluated through a Monte Carlo simulation study. Furthermore, we are committed to investigating three widely recognized risk metrics: the value at risk, the tail value at risk, and the tail variance premium. These findings are helpful for actuarial risk researchers who depend on risk measurement fitting when evaluating Bayesian tools for effectively modeling actuarial sciences. Finally, different applications taken from several areas are examined to illustrate the practical usefulness of the compound Rayleigh exponential distribution. Using various model selection criteria, the introduced model is contrasted with that of several well-known distributions. Our empirical findings indicate that the suggested model has superior goodness-of-fit to the other models examined.

**OPEN ACCESS**

**Received:** 22/09/2025

**Accepted:** 28/10/2025

**Published:** 30/12/2025

**DOI**
10.23967/j.rimni.2025.10.73596

**Keywords:**
Applied sciences
Bayesian estimation
insurance
loss functions
maximum product spacing
Monte Carlo simulation

## 1 Introduction

Numerous fields make extensive use of statistical distributions to model various types of data, including complex, skewed (left and right), symmetric, asymmetric, and bimodal data. They have been

*Correspondence: Hassan Alsuhabi (hrsuhabi@uqu.edu.sa). This is an article distributed under the terms of the Creative Commons BY-NC-SA license

applied in diverse areas such as lifetime analysis, reliability, insurance, engineering, finance, economics, biology, extreme events, medicine, agriculture, actuarial science, demography, sports, and materials science, among others. Consequently, there is a demand for generalized forms of these existing distributions to capture such data better. This demand has led authors to develop new modifications to existing distributions, incorporating one or more additional parameters to increase their flexibility. Moreover, this class of distributions plays a significant role in survival analysis and reliability theory. Another important aspect of these models is their ability to effectively describe natural phenomena. Their value spans several domains, notably engineering, industrial applications, biology, medical science, actuarial science, and insurance. Taking a different approach, Marshall and Olkin [1] introduced a new family of distributions by adding a parameter to the classical distribution. Mahdavi and Kundu [2] introduced a new method to add an extra parameter to the baseline distributions. El-Morshedy et al. [3] defined a novel tool to fit medical data. This novel statistical approach is referred to as a modified family of distributions. Furthermore, Alshanbari et al. [4] provided the E-X method by adding one additional parameter to the classical model, Ahmad et al. [5] defined the loss technique that transforms the baseline distribution to solve the constraints of existing models by increasing modeling flexibility for several types of data sets. ElSherpieny and Almetwally [6] discussed the exponentiated generalized alpha power family. Bashiru et al. [7] introduced the hybrid cosine inverse Lomax-G family of distributions and applied it to medical and engineering data. Sadia et al. [8] studied the truncated life tests for the Kumaraswamy Bell-Rayleigh distribution. Similarly, various authors have investigated analogous approaches for alternative distributions. This includes the work of Meraou et al. [9–12], Almetwally and Meraou [13], Alyami et al. [14], Ahmad et al. [15], Aldahlan et al. [16], Almarashi et al. [17], Al-Moisheer et al. [18], Benchiha et al. [19], Orji et al. [20], Saboor et al. [21], Sapkota et al. [22], Eugene et al. [23], Moakof et al. [24], Azzalini [25], Thomas and Chacko [26], Hammad et al. [27], Hassan et al. [28], Chinedu et al. [29], and references cited therein.

In most scenarios, the Rayleigh model holds significant value for examining real-world data across diverse sectors such as engineering, finance, healthcare, and telecommunications. It is a particular example of the generalized extreme value distribution. Several studies of the Rayleigh distribution have been considered. Among these models, Bashiru et al. [30] defined the cosine Rayleigh model, the type-I heavy-tailed Rayleigh distribution was discussed by Nwankwo et al. [31]. The probability density function (PDF), cumulative distribution function (CDF), and cumulative hazard function (chf) of a random variable $W_1$, are written, respectively, as follows:

$$k_1(w_1;\delta) = 2\delta w_1\, e^{-\delta w_1^2}, \quad w_1 > 0,\ \delta > 0,$$

$$K_1(w_1;\delta) = 1 - e^{-\delta w_1^2},$$

and

$$\mathrm{chf}_1(w_1,\delta) = \delta w_1^2. \tag{1}$$

To our knowledge, the one-parameter exponential distribution has wider applications in biology, medical sciences, health sciences, and other fields. It is frequently applied to fit the upper tail of disease severity data, which is essential for identifying worst-case scenarios in epidemiological studies. The exponential model has received a lot of attention, for example, see Alghamd et al. [32], Afify et al. [33], and Hassan et al. [34]. For this, let $W_2$ be a random variable that follows the exponential model with parameter $\eta$. Then, the PDF, CDF, and chf, can be expressed, respectively, as follows:

$$k_2(w_2;\eta) = \eta\, e^{-\eta w_2}, \quad w_2 > 0,\ \eta > 0,$$

$$K_2(w_2;\eta) = 1 - e^{-\eta w_2},$$

and

$$\mathrm{chf}_2(w_2,\eta) = \eta w_2. \tag{2}$$

Hussein et al. [35] introduced a novel distribution called the compound Rayleigh exponential distribution (CRED) with two parameters. It maintains the original distributions while providing more flexibility and accuracy when modeling the data. Motivated by the above comprehensive discussion, in this article, we present several estimation techniques of the CRED parameters using various Bayesian and non-Bayesian estimation methods, including the maximum likelihood estimator, the maximum product of spacings estimator, least square estimator, weighted least square estimator, Cramer-Von-Mise estimator, Anderson-Darling estimator, and Bayesian methods with informative and non informative priors under square error, Linex, and general entropy loss function. Additionally, we construct various types of confidence intervals for the model parameters by applying approximate and Bootstrap methods. For more details, see Saeid et al. [36], Abdelall et al. [37], AL-Dayian et al. [38], Sadiah and Aljeddani [39], Al-Babtain et al. [40], and Marwan and Basim [41], and Dutta et al. [42–47]. In addition, we applied practical data applications to demonstrate the significance of the CRED in real-world contexts. The proposed data sets are obtained from the radiotherapy and industrial fields. This research, by utilizing a range of evaluation metrics, demonstrates substantial proof that the CRED may serve as a viable option for examining and interpreting real-world occurrences in various domains. In addition, we are motivated in this study to examine three risk measures for the suggested CRED, notably the value at risk metric (VaR), tail value at risk metric (TVaR), and tail variance premium (TVP) metric.

A random variable $W$ is said to have the CRED if its CDF is

$$G(w,\delta,\eta) = 1 - e^{-\delta w^2 - \eta w}, \quad w > 0;\ \delta,\ \eta > 0. \tag{3}$$

The corresponding PDF of $W$ is given by

$$g(w,\delta,\eta) = (2\delta w + \eta)\, e^{-\delta w^2 - \eta w}. \tag{4}$$

Fig. 1 illustrates the plot for the CRED. The illustrations shown in Fig. 1 are arranged across various plots:

- The first behavior of $g(w,\delta,\eta)$ is illustrated in Fig. 1a,c, corresponding to $\delta = 0.25$ and $\eta = 0.5$, and $\delta = 0.5$ and $\eta = 2.4$. This illustrates the combined influence of $\delta$ and $\eta$ on the configuration of $g(w,\delta,\eta)$, resulting in a decreasing shape.
- Fig. 1d depicts the second potential behavior of $g(w,\delta,\eta)$, which is associated with $\delta = 3.2$ and $\eta = 1.7$. This representation highlights the joint impact of $\delta$ and $\eta$ on the form of $g(w,\delta,\eta)$, leading to an unimodal shape.
- Illustrated in Fig. 1b is the first possible behavior of $g(w,\delta,\eta)$, which aligns with $\delta = 1.8$ and $\eta = 0.3$. This demonstrates how $\delta$ and $\eta$ collectively influence the structure of $g(w,\delta,\eta)$, resulting in a right-skewed shape.

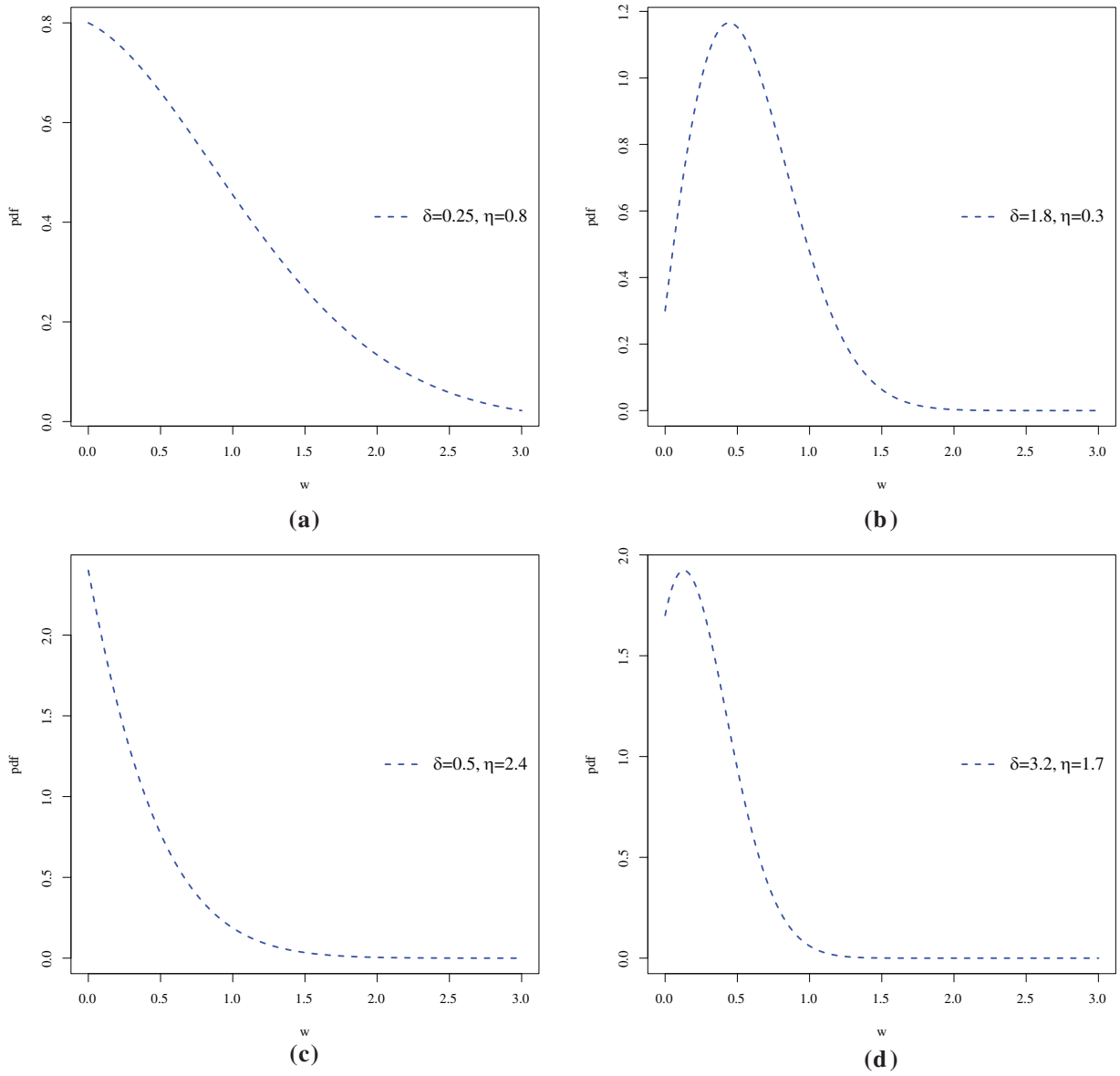


**Figure 1:** PDF plots of the CRED model (a) $(\delta, \eta) = (0.25, 0.8)$; (b) $(\delta, \eta) = (1.8, 0.3)$; (c) $(\delta, \eta) = (0.5, 2.4)$; (d) $(\delta, \eta) = (3.2, 1.7)$

The survival function (SF) and hazard rate function (HRF) of the random variable $W$ are given by

$$S(w; \delta, \eta) = e^{-\delta w^2 - \eta w}$$

and

$$h(w; \delta, \eta) = 2\delta\, w + \eta.$$

Fig. 2 shows some graphical representations of the HRF of the CRED. The illustrations depicted in Fig. 2 are distributed over different plots:

- These plots demonstrate potential behavior of $h(w;\delta,\eta)$, associated with all proposed parameter values of $\delta$ and $\eta$. These illustrations highlight the joint influence of $\delta$ and $\eta$ on the configuration of $h(w;\delta,\eta)$, leading to an increasing shape.

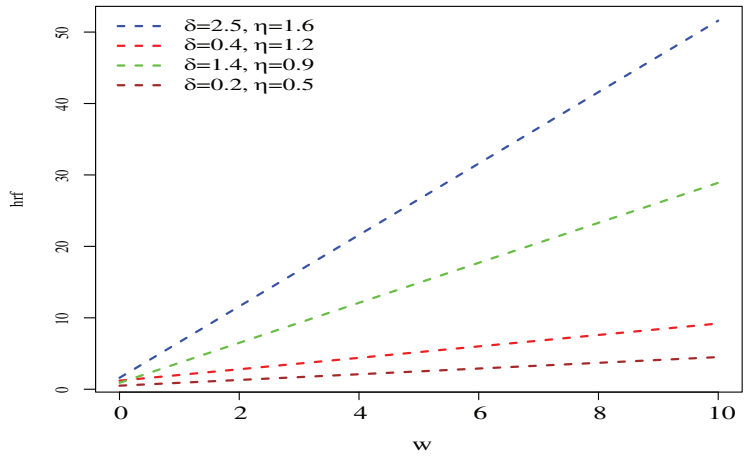


**Figure 2:** HRF plots of the CRED model

## 2 Parameter Estimation Inference

### *2.1 Maximum Likelihood Estimation Method*

Let $W_1, W_2, \ldots, W_m$ be a random sample of size $m$ drawn from the PDF given in Eq. (4). The log-likelihood function can be represented as:

$$\mathcal{LL}(w,\delta,\eta) = \sum_{i=1}^{m} \log(2\delta w_i^2 + \eta) - \delta \sum_{i=1}^{m} w_i^2 - \eta \sum_{i=1}^{m} w_i \tag{5}$$

To obtain the MLEs of parameters $\delta$ and $\eta$, denoted by $\mathcal{S}_1$, we differentiate Eq. (5) with respect to the parameters $\delta$ and $\eta$. These derivatives are identified as:

$$\frac{\partial \mathcal{LL}(w,\delta,\eta)}{\partial \delta} = \sum_{i=1}^{m} \frac{2w_i^2}{2\delta w_i^2 + \eta} - \sum_{i=1}^{m} w_i^2, \tag{6}$$

and

$$\frac{\partial \mathcal{LL}(w,\delta,\eta)}{\partial \eta} = \sum_{i=1}^{m} \frac{1}{2\delta w_i^2 + \eta} - \sum_{i=1}^{m} w_i. \tag{7}$$

To find the MLE of $\delta$ and $\eta$, let's say $\mathcal{S}_1$, the above non-linear equations must be solved. Since these equations cannot be solved analytically, numerical methods must be used. Iterative techniques, such as the Newton-Raphson algorithm, can be employed to compute the final estimates of $\delta$ and $\eta$ using statistical software.

### *2.2 Maximum Product of Spacings Method*

The MPS is the most frequently used method of parameter estimation. It enjoys many desirable properties, including consistency, asymptotic efficiency, and the invariance property, as well as its

intuitive appeal. The MPS method was first proposed by Cheng and Amin [48]. It aims to maximize the product of spacing, the differences between successive values of the theoretical CDF evaluated at the ordered data points. The MPS is based on the geometric mean of the spacings, which are defined as:

$$M_i(\delta,\eta) = G(w_{(i)};\delta,\eta) - G(w_{(i-1)};\delta,\eta), i = 1,\ldots,m+1,$$

where, $G(w_{(0)};\delta,\eta) = 0$ and $G(w_{(m+1)};\delta,\eta) = 1$. As a result, the product of the spacings satisfies: $\sum_{i=1}^{m+1} M_i(\delta,\eta) = 1$.

Hence, the MPS estimators of $\delta$ and $\eta$, say $\mathcal{S}_2$ are computed by maximizing the geometric mean of the spacing

$$\mathcal{S}_2 = \left[\prod_{i=1}^{m+1} M_i(\delta,\eta)\right]^{\frac{1}{m+1}}. \tag{8}$$

### *2.3 Least Squares Estimator*

The function denoted by $\mathcal{S}_3$ represents the squared distance between the empirical and theoretical CDFs, which is minimized to obtain the least squares estimates of $\delta$ and $\eta$ for the CRED.

$$\begin{aligned}\mathcal{S}_3 &= \sum_{i=1}^{m}\left[G(w_{(i)};\delta,\eta) - \frac{i}{m+1}\right]^2 \\ &= \sum_{i=1}^{m}\left[1 - e^{-\delta w_{(i)}^2 - \eta w_{(i)}} - \frac{i}{m+1}\right]^2.\end{aligned}$$

### *2.4 Weighted Least Squares Estimator*

To obtain the weighted least squares estimates of $\delta$ and $\eta$, denoted by $\mathcal{S}_4$, a modified version of the above function is minimized, as shown below:

$$\begin{aligned}\mathcal{S}_4 &= \sum_{i=1}^{m}\frac{(m+1)^2(m+2)}{(m+1-i)i}\left[G(w_{(i)};\delta,\eta) - \frac{i}{m+1}\right]^2 \\ &= \sum_{i=1}^{m}\frac{(m+1)^2(m+2)}{(m+1-i)i}\left[1 - e^{-\delta w_{(i)}^2 - \eta w_{(i)}} - \frac{i}{m+1}\right]^2.\end{aligned}$$

### *2.5 Minimum Distance Methods*

Several procedures are introduced for minimizing the empirical and estimated distribution functions. In this study, the CVE and ADE tools are used.

For the CVE estimators, the function denoted by $\mathcal{S}_5$ will be minimized for getting the estimates of CRED parameters $\delta$ and $\eta$. The required function is defined as:

$$\mathcal{S}_5 = \frac{1}{12m} + \sum_{i=1}^{m}\left[G(w_{(i)};\delta,\eta) - \frac{2i-1}{2m}\right]^2$$
$$= \frac{1}{12m} + \sum_{i=1}^{m}\left[1 - e^{-\delta w_{(i)}^2 - \eta w_{(i)}} - \frac{2i-1}{2m}\right]^2.$$

Next, the ADE procedure uses the following approach for estimation of the parameter by giving the CDF function of the distribution and minimizing the following function:

$$\mathcal{S}_6 = -m - \frac{1}{m}\sum_{m=1}^{m}(2m-1)\left\{\log[G(w_{(i:n)};\delta,\eta)] + \log[1 - G(w_{(i)};\delta,\eta)]\right\}$$
$$= -m - \frac{1}{m}\sum_{m=1}^{m}(2m-1)\left\{\log\left[1 - e^{-\delta w_{(i)}^2 - \eta w_{(i)}}\right] - \left[\delta w_{(i)}^2 + \eta w_{(i)}\right]\right\}.$$

### *2.6 Bayesian Method*

#### *2.6.1 Bayesian Estimation Concerning Informative Priors*

Let $\delta$ and $\eta$ be random variables that take a gamma distribution with PDFs given, respectively, by

$$\pi_1(\delta) = \frac{d_1^{c_1}}{\Gamma(c_1)}\,\delta^{c_1-1}\,e^{-d_1\delta}, \quad \delta, d_1, c_1 > 0$$

and

$$\pi_2(\eta) = \frac{d_2^{c_2}}{\Gamma(c_2)}\,\eta^{c_2-1}\,e^{-d_2\eta}, \quad \eta, d_2, c_2 > 0.$$

Hence, for $\Xi = (\delta, \eta)$ the joint prior PDF is

$$\pi(\Xi) \propto \delta^{c_1-1}\,\eta^{c_2-1}\,e^{-d_1\delta - d_2\eta}.$$

The joint prior PDF of $\Xi$ can be written below

$$\pi^*(\Xi \mid w) = \mathcal{L}(\delta,\eta)\pi(\Xi)$$
$$= \delta^{c_1-1}\,\eta^{c_2-1}\,e^{-d_1\delta - d_2\eta}\prod_{i=1}^{m}(2\delta w_i + \eta)\,e^{-\delta w_i^2 - \eta w_i}.$$

#### *2.6.2 Bayesian Estimation with Respect to Non-Informative Priors*

Here, we assume that the parameters $\delta$ and $\eta$ have the uniform prior with interval (0, 1). Consequently, the prior PDFs of $\delta$ and $\eta$ are

$$\pi_1(\delta) = 1, \quad 0 < \delta < 1,$$

and

$$\pi_1(\eta) = 1, \quad 0 < \eta < 1.$$

Thus, the associated joint prior PDFs of $\delta$ and $\eta$ can be written as

$$\pi(\Xi) \propto 1.$$

At the end, we can deduce the posterior density of $\delta$ and $\eta$, and it can be established by

$$\pi^*(\Xi \mid w) = \mathcal{L}(\Xi))\pi(\Xi \mid w)$$
$$= \prod_{i=1}^{m}(2\delta w_i + \eta)\, e^{-\delta w_i^2 - \eta w_i}.$$

Now, we assume that $\delta$ and $\eta$ follow Jeffreys priors [49,50], which are proportional to the square root of the Fisher information matrix:

$$p(\Xi) \propto \sqrt{I(\Xi)},$$

where, $I(\Xi) = -E\left[\dfrac{\partial^2 g(w;\Xi)}{\partial \Xi^2}\right]$ represents the Fisher information matrix. Let the parameters $\delta$ and $\eta$ follow, respectively, the prior PDFs defined by

$$\pi_1(\delta) = \frac{1}{\delta}, \quad \delta > 0$$

and

$$\pi_1(\eta) = \frac{1}{\eta}, \quad \eta > 0.$$

As a result, the joint prior PDF is

$$\pi(\Xi) \propto \frac{1}{\delta\eta}.$$

Further, the posterior density can be given as

$$\pi^*(\Xi \mid w) = \mathcal{L}(\Xi))\pi(\Xi \mid w)$$
$$= (\delta\eta)^{-m}\prod_{i=1}^{m}(2\delta w_i + \eta)\, e^{-\delta w_i^2 - \eta w_i}.$$

At the end, the Bayes estimator based square error loss function (SELF)

$$Q = (\Xi - \hat{\Xi})^2$$

is obtained to be

$$\hat{Q}_{SELF} = \int_{\Xi} Q\, \pi^*(\Xi \mid w)\, d\Xi. \tag{9}$$

In the same line, the Bayes estimator based on the Linex loss function (LILF) $Q = e^{s(\Xi-\hat{\Xi})} - s(\Xi - \hat{\Xi})$ is

$$\hat{Q}_{LILF} = -\frac{1}{s}\ln\left(\int_{\Xi} e^{-sQ}\, \pi^*(\Xi \mid w)\, d\Xi\right). \tag{10}$$

Finally, under general entropy loss function (GELF) $Q = \left(\frac{\hat{\Xi}}{\Xi}\right)^s - s\ln\left(\frac{\hat{\Xi}}{\Xi}\right) - 1$, the Bayes estimator can be given by

$$\hat{Q}_{GELF} = \left(\int_{\Xi} Q^{-s}\, \pi^*(\Xi \mid w)\, d\Xi\right)^{-1/s}, \tag{11}$$

with $s \neq 0$. It is well known that the integrals derived from the Bayes estimators under all proposed loss functions cannot be computed analytically. For this, the Markov Chain Monte Carlo (MCMC) method based on the Metropolis-Hasting (MH) process is used to find an approximation of the integral values in Eqs. (9)–(11). The steps of the proposed MH process can be described as follows

- Started $(\delta, \eta)$ as $(\delta^0, \eta^0)$.
- Put $i = 1$.
- Generate the random sample for $\delta^*$ and $\eta^*$ as

  $\delta \sim LN(\delta^i, \psi_{11})$, and $\quad \eta \sim LN(\eta^i, \psi_{22})$,

  with $\psi_{ij}$ represents the element of the variance-covariance matrix.
- Compute the statistics $Z_\delta = \min\left[1, \dfrac{\pi^*(\delta^* \mid \eta^{i-1})}{\pi^*(\delta^{i-1} \mid \eta^{i-1})}\right]$ and $Z_\eta = \min\left[1, \dfrac{\pi^*(\eta^* \mid \delta^{i-1})}{\pi^*(\eta^{i-1} \mid \delta^{i-1})}\right]$.
- A random sample $Z_i$ is drawn from U(0,1), for $i = 1, 2$.
- If $W_1 \leq T_\delta,\ W_2 \leq T_\eta$ then $\delta^i = \delta^*,\ \eta^i = \eta^*$ else $\delta^i = \delta^{i-1},\ \eta^i = \eta^{i-1}$.
- $i = i + 1$.
- The steps 3–6, are repeated $N$ times to result a random samples $\delta^i$, and $\eta^i$.

Now, to delete the issue of the initial guess, we delete $N'$ initial samples (burn-in period). Furthermore, we can compute the credible intervals by applying the idea of Chen and Shao [51], and generating posterior samples (Cred Int). Consequently, the $100(1-\alpha)\%$ Cred Int of $\Xi = (\delta, \eta)$ is defined by

$$\frac{1}{N^*}\sum_{j=i_1^*}^{N^*} \Xi_{(j)} \leq 1 - \alpha \leq \frac{1}{N^*}\sum_{j=i_1^*}^{N^*} \Xi_{(j)}, \tag{12}$$

where, $i_1^* < i_2^*,\ i_1^*, i_2^* \in \{1, 2, \ldots, N\}$ and $N^* = N - N'$.

### *2.7 Interval Estimation Method*

In this subsection, we investigate three approximate methods for constructing confidence intervals (CIs) for the unknown parameters $\delta$ and $\eta$

#### *2.7.1 Asymptotic CI*

The asymptotic distribution of MLEs for $\Xi = (\delta, \eta)$ can be written as follows

$$\left(\hat{\Xi} - \Xi\right) \sim \mathbf{N}(0, \mathbf{V}^{-1}(\Xi)),$$

where $\mathbf{V}^{-1}(\Xi)$ denotes the variance-covariance matrix for $\Xi$, and its elements are

$$\mathbf{V}(\Xi) = -\begin{pmatrix} \dfrac{\partial^2 \mathcal{LL}(\Xi)}{\partial \delta^2} & \dfrac{\partial^2 \mathcal{LL}(\Xi)}{\partial \delta \partial \eta} \\ \dfrac{\partial^2 \mathcal{LL}(\Xi)}{\partial \delta \partial \eta} & \dfrac{\partial^2 \mathcal{LL}(\Xi)}{\partial \eta^2} \end{pmatrix}$$

So, the $100(1-\alpha)\%$ approximate CI for $\Xi$ can be obtained as

$$(\hat{\Xi}_i \pm N_{1-\alpha/2}\sqrt{\mathbf{V}_{ii}^{-1}}), \quad i = 1, 2,$$

with $N_{1-\alpha/2}$ follows N(0, 1).

### 2.7.2 *Bootstrap CI*

This subsection discusses two bootstrap techniques for constructing the CIs for $\delta$ and $\eta$. The proposed methods are the Bootstrap-percentile (boot-p) and Bootstrap-t (boot-t). The two tools can be described as

(A) Boot-p algorithm

1. Under the obtain complete random sample using the actual parameter values $\Xi$, we obtain the final estimate $\hat{\Xi}$.
2. By applying $\hat{\Xi}$ as the initial parameter, we obtain the estimate $\hat{\Xi}^*$.
3. The step 2 repeated $M$ times.
4. Suppose $\hat{G}_1(w) = P(\hat{\Xi}^* \leq w)$, so we calculate $\hat{\Xi}_M(w) = \hat{G}_1^{-1}(w)$. An approximate $100(1-\alpha)\%$CI for $\Xi$ is now given by

$$\left(\hat{\Xi}^*_M\left(\frac{\alpha}{2}\right), \hat{\Xi}^*_M\left(1-\frac{\alpha}{2}\right)\right).$$

(B) Boot-t algorithm

1. By applying the boot-p procedure, we compute $\hat{\Xi}^*$.
2. Find $J = \dfrac{\hat{\Xi}^* - \tilde{\Xi}}{\sqrt{\mathbf{V}(\hat{\Xi}^*)}}$.
3. The step 2 repeated $M$ times.
4. Suppose $\hat{G}_2(w) = P(\tilde{J} \leq w)$, so we calculate $\hat{\Xi}_M(w) = \hat{\Xi} + \sqrt{\mathbf{V}(\hat{\Xi})}\hat{G}_2^{-1}(w)$. Further, the approximate $100(1-\alpha)\%$ CI for $\Xi$ is evaluated as

$$\left(\hat{\Xi}^*_M\left(\frac{\alpha}{2}\right), \hat{\Xi}^*_M\left(1-\frac{\alpha}{2}\right)\right).$$

## 3 Simulation Study

This section presents a Monte Carlo (MC) simulation study to evaluate the performance of the proposed estimation methods for the CRED. For simulation analysis, we generate a random sample from the CRED using its quantile function given as

$$w_u = \frac{-\eta + \sqrt{4\delta \log(1-u)}}{2\delta}, \quad 0 < u < 1.$$

Two sets of different combinations of parameter values of the CRED, such as $\Xi = (\delta, \eta)$ (set 1: (0.3, 0.7), and set 2: (1.1, 1.3), are employed. It is important to note that no strict assumptions were made regarding the selection of parameter values in the simulation study. Random samples of sizes, say, $m = \{25, 50, 75, 100\}$ are generated from CRED, and the whole process for each sample is repeated 2000 times. We considered the mean estimates (AEs), average bias (ABs), and mean squared error (MSEs) as the pivotal tools to examine the performance of the proposed estimation techniques. The simulation process uses the R language software with the optim function. The numerical results of the simulation analysis are presented in Tables 1–6. To ensure convergence of the MCMC procedures,

we plotted the histogram, trace plots, autocorrelation function (ACF), and Gelman–Rubin diagnostics for the unknown parameters $\delta$ and $\eta$. The proposed curves are reported in Figs. 3–6.

**Table 1:** Numerical Simulation experiment of the CRED using set 1

| $m$ | | $\delta$ | | | | | $\eta$ | | | | |
|---|---|---|---|---|---|---|---|---|---|---|---|
| | | $\mathcal{S}_1$ | $\mathcal{S}_2$ | Bayes (informative prior) | | | $\mathcal{S}_1$ | $\mathcal{S}_2$ | Bayes (informative prior) | | |
| | | | | SELF | LILF | GELF | | | SELF | LILF | GELF |
| 25 | AE | 0.4290 | 0.2515 | 0.2066 | 0.2367 | 0.2176 | 0.6441 | 0.6933 | 0.7745 | 0.8039 | 0.8153 |
| | AB | 0.1290 | 0.0485 | 0.0934 | 0.0573 | 0.0564 | 0.0559 | 0.0067 | 0.0745 | 0.0536 | 0.1257 |
| | MSE | 0.0884 | 0.0545 | 0.0195 | 0.0197 | 0.0198 | 0.1226 | 0.1259 | 0.0279 | 0.0283 | 0.0287 |
| 50 | AE | 0.4802 | 0.2681 | 0.3595 | 0.3404 | 0.3574 | 0.6756 | 0.7309 | 0.7526 | 0.7512 | 0.7390 |
| | AB | 0.0645 | 0.0319 | 0.0595 | 0.0446 | 0.0713 | 0.0244 | 0.0309 | 0.0526 | 0.0545 | 0.0497 |
| | MSE | 0.0301 | 0.0213 | 0.0107 | 0.0109 | 0.0111 | 0.0445 | 0.0484 | 0.0158 | 0.0161 | 0.0164 |
| 75 | AE | 0.3107 | 0.2728 | 0.3174 | 0.3149 | 0.3175 | 0.7149 | 0.7371 | 0.7187 | 0.7007 | 0.7176 |
| | AB | 0.0107 | 0.0272 | 0.0174 | 0.0197 | 0.0384 | 0.0149 | 0.0371 | 0.0187 | 0.0060 | 0.0305 |
| | MSE | 0.0211 | 0.0210 | 0.0042 | 0.0044 | 0.0047 | 0.0318 | 0.0446 | 0.0051 | 0.0054 | 0.0056 |
| 100 | AE | 0.3177 | 0.2806 | 0.2945 | 0.3247 | 0.3317 | 0.6921 | 0.7258 | 0.7230 | 0.7017 | 0.6963 |
| | AB | 0.0177 | 0.0194 | 0.0183 | 0.0288 | 0.0402 | 0.0079 | 0.0258 | 0.0230 | 0.0056 | 0.0012 |
| | MSE | 0.0118 | 0.0129 | 0.0026 | 0.0029 | 0.0030 | 0.0228 | 0.0238 | 0.0038 | 0.0041 | 0.0042 |

**Table 2:** Numerical Simulation experiment of the CRED using set 1

| $m$ | Method | $\delta$ | | | $\eta$ | | |
|---|---|---|---|---|---|---|---|
| | | AE | AB | MSE | AE | AB | MSE |
| 25 | $\mathcal{S}_3$ | 0.2974 | 0.0026 | 0.0793 | 0.7372 | 0.0372 | 0.0859 |
| | $\mathcal{S}_4$ | 0.3143 | 0.0143 | 0.0879 | 0.7469 | 0.0469 | 0.1084 |
| | $\mathcal{S}_5$ | 0.3493 | 0.0493 | 0.1015 | 0.6989 | 0.0011 | 0.1277 |
| | $\mathcal{S}_6$ | 0.3541 | 0.0541 | 0.0828 | 0.6821 | 0.0179 | 0.0926 |
| 50 | $\mathcal{S}_3$ | 0.2983 | 0.0017 | 0.0282 | 0.7155 | 0.0155 | 0.0534 |
| | $\mathcal{S}_4$ | 0.3035 | 0.0035 | 0.0283 | 0.7037 | 0.0037 | 0.0652 |
| | $\mathcal{S}_5$ | 0.3161 | 0.0161 | 0.0448 | 0.7105 | 0.0105 | 0.072 |
| | $\mathcal{S}_6$ | 0.3091 | 0.0091 | 0.0388 | 0.7032 | 0.0032 | 0.0789 |
| 75 | $\mathcal{S}_3$ | 0.3043 | 0.0043 | 0.0266 | 0.6827 | 0.0173 | 0.0403 |
| | $\mathcal{S}_4$ | 0.3194 | 0.0194 | 0.0268 | 0.7071 | 0.0071 | 0.0482 |
| | $\mathcal{S}_5$ | 0.3204 | 0.0204 | 0.0284 | 0.7113 | 0.0113 | 0.0432 |

(Continued)

**Table 2 (continued)**

| $m$ | Method | $\delta$ | | | $\eta$ | | |
|---|---|---|---|---|---|---|---|
| | | AE | AB | MSE | AE | AB | MSE |
| | $\mathcal{S}_6$ | 0.2967 | 0.0033 | 0.0190 | 0.7184 | 0.0184 | 0.0296 |
| 100 | $\mathcal{S}_3$ | 0.299 | 0.001 | 0.0165 | 0.7088 | 0.0088 | 0.0282 |
| | $\mathcal{S}_4$ | 0.317 | 0.017 | 0.0166 | 0.6851 | 0.0149 | 0.0272 |
| | $\mathcal{S}_5$ | 0.3277 | 0.0277 | 0.0229 | 0.7055 | 0.0055 | 0.0271 |
| | $\mathcal{S}_6$ | 0.3217 | 0.0217 | 0.0168 | 0.6959 | 0.0041 | 0.0279 |

**Table 3:** Numerical Simulation experiment of the CRED using set 2

| $m$ | | $\delta$ | | | | | $\eta$ | | | | |
|---|---|---|---|---|---|---|---|---|---|---|---|
| | | $\mathcal{S}_1$ | $\mathcal{S}_2$ | Bayes (informative prior) | | | $\mathcal{S}_1$ | $\mathcal{S}_2$ | Bayes (informative prior) | | |
| | | | | SELF | LILF | GELF | | | SELF | LILF | GELF |
| | AE | 1.3617 | 1.1583 | 1.0455 | 1.0274 | 1.0411 | 1.1765 | 1.3522 | 1.2838 | 1.3017 | 1.3142 |
| 25 | AB | 0.2617 | 0.0583 | 0.0545 | 0.0688 | 0.0554 | 0.1235 | 0.0522 | 0.0162 | 0.0325 | 0.0223 |
| | MSE | 0.7883 | 0.8648 | 0.0295 | 0.0297 | 0.0299 | 0.4132 | 0.4265 | 0.0237 | 0.0239 | 0.0241 |
| | AE | 1.2681 | 1.1921 | 1.0943 | 1.0710 | 1.0716 | 1.2491 | 1.2251 | 1.3277 | 1.3428 | 1.3413 |
| 50 | AB | 0.1681 | 0.0921 | 0.0057 | 0.0152 | 0.0094 | 0.0509 | 0.0749 | 0.0212 | 0.0451 | 0.0538 |
| | MSE | 0.3312 | 0.3813 | 0.0107 | 0.0108 | 0.0110 | 0.1282 | 0.2120 | 0.0155 | 0.0157 | 0.0159 |
| | AE | 1.1885 | 1.1319 | 1.1206 | 1.1325 | 1.1323 | 1.2961 | 1.3470 | 1.3416 | 1.3564 | 1.3503 |
| 75 | AB | 0.0885 | 0.0319 | 0.0206 | 0.0362 | 0.0415 | 0.0039 | 0.0470 | 0.0416 | 0.0668 | 0.0565 |
| | MSE | 0.2198 | 0.2419 | 0.0133 | 0.0136 | 0.0137 | 0.1217 | 0.1478 | 0.0143 | 0.0145 | 0.0147 |
| | AE | 1.1068 | 1.0935 | 1.1199 | 1.1304 | 1.1474 | 1.3343 | 1.3019 | 1.3112 | 1.3068 | 1.2962 |
| 100 | AB | 0.0068 | 0.0065 | 0.0199 | 0.0348 | 0.0589 | 0.0343 | 0.0019 | 0.0112 | 0.0099 | 0.0072 |
| | MSE | 0.1606 | 0.1901 | 0.0089 | 0.0091 | 0.0093 | 0.1060 | 0.1199 | 0.0063 | 0.0065 | 0.0067 |

**Table 4:** Numerical Simulation experiment of the CRED using set 2

| $m$ | Method | $\delta$ | | | $\eta$ | | |
|---|---|---|---|---|---|---|---|
| | | AE | AB | MSE | AE | AB | MSE |
| 25 | $\mathcal{S}_3$ | 1.1852 | 0.0852 | 1.316 | 1.3581 | 0.0581 | 0.5121 |
| | $\mathcal{S}_4$ | 1.2416 | 0.1416 | 1.465 | 1.2113 | 0.0887 | 0.3656 |
| | $\mathcal{S}_5$ | 1.2719 | 0.1719 | 1.0389 | 1.2716 | 0.0284 | 0.4135 |
| | $\mathcal{S}_6$ | 1.1670 | 0.0670 | 0.9684 | 1.3376 | 0.0376 | 0.4967 |
| 50 | $\mathcal{S}_3$ | 1.0578 | 0.0422 | 0.5569 | 1.3162 | 0.0162 | 0.2076 |
| | $\mathcal{S}_4$ | 1.1933 | 0.0933 | 0.4410 | 1.2350 | 0.0650 | 0.1479 |
| | $\mathcal{S}_5$ | 1.1881 | 0.0881 | 0.5097 | 1.2597 | 0.0403 | 0.1709 |

(Continued)

**Table 4 (continued)**

| $m$ | Method | $\delta$ | | | $\eta$ | | |
|---|---|---|---|---|---|---|---|
| | | AE | AB | MSE | AE | AB | MSE |
| | $\mathcal{S}_6$ | 1.1277 | 0.0277 | 0.3727 | 1.2814 | 0.0186 | 0.2489 |
| 75 | $\mathcal{S}_3$ | 1.0696 | 0.0304 | 0.2804 | 1.3190 | 0.0190 | 0.1248 |
| | $\mathcal{S}_4$ | 1.1617 | 0.0617 | 0.3476 | 1.3032 | 0.0032 | 0.1623 |
| | $\mathcal{S}_5$ | 1.1976 | 0.0976 | 0.4074 | 1.2607 | 0.0393 | 0.1474 |
| | $\mathcal{S}_6$ | 1.1878 | 0.0878 | 0.2258 | 1.2486 | 0.0514 | 0.1350 |
| 100 | $\mathcal{S}_3$ | 1.0122 | 0.0878 | 0.1947 | 1.3323 | 0.0323 | 0.0985 |
| | $\mathcal{S}_4$ | 1.1308 | 0.0308 | 0.1817 | 1.3096 | 0.0096 | 0.0791 |
| | $\mathcal{S}_5$ | 1.1686 | 0.0686 | 0.3571 | 1.2711 | 0.0289 | 0.1364 |
| | $\mathcal{S}_6$ | 1.1705 | 0.0705 | 0.1570 | 1.2462 | 0.0538 | 0.0836 |

**Table 5:** Numerical Simulation experiment of the CRED using set 1 (non-informative prior)

| $m$ | | $\delta$ | | | $\eta$ | | |
|---|---|---|---|---|---|---|---|
| | | AE | AB | MSE | AE | AB | MSE |
| 25 | SELF | 0.4239 | 0.1239 | 0.0264 | 0.6349 | 0.0650 | 0.0265 |
| | LILF | 0.4211 | 0.1211 | 0.0266 | 0.6294 | 0.0706 | 0.0267 |
| | GELF | 0.3997 | 0.1239 | 0.0268 | 0.6077 | 0.1077 | 0.0269 |
| 50 | SELF | 0.3408 | 0.0408 | 0.0109 | 0.7608 | 0.0608 | 0.0157 |
| | LILF | 0.3397 | 0.0397 | 0.0111 | 0.7594 | 0.0594 | 0.0159 |
| | GELF | 0.3303 | 0.0303 | 0.0113 | 0.7551 | 0.0551 | 0.0161 |
| 75 | SELF | 0.3481 | 0.0481 | 0.0059 | 0.7058 | 0.0058 | 0.0061 |
| | LILF | 0.3472 | 0.0472 | 0.0061 | 0.7050 | 0.0050 | 0.0063 |
| | GELF | 0.3397 | 0.0397 | 0.0063 | 0.7023 | 0.0023 | 0.0065 |
| 100 | SELF | 0.3188 | 0.0188 | 0.0036 | 0.7353 | 0.0353 | 0.0042 |
| | LILF | 0.3185 | 0.0185 | 0.0038 | 0.7348 | 0.0348 | 0.0044 |
| | GELF | 0.3158 | 0.01587 | 0.0040 | 0.7332 | 0.0332 | 0.0045 |

**Table 6:** Numerical Simulation experiment of the CRED using set 2 (non-informative prior)

| $m$ | | $\delta$ | | | $\eta$ | | |
|---|---|---|---|---|---|---|---|
| | | AE | AB | MSE | AE | AB | MSE |
| 25 | SELF | 1.1139 | 0.0139 | 0.0361 | 1.2697 | 0.0302 | 0.0326 |
| | LILF | 1.1124 | 0.0124 | 0.0363 | 1.2668 | 0.0332 | 0.0328 |
| | GELF | 1.1098 | 0.0098 | 0.0365 | 1.2629 | 0.0371 | 0.0329 |
| 50 | SELF | 1.1562 | 0.0562 | 0.0265 | 1.3734 | 0.0734 | 0.0171 |
| | LILF | 1.1554 | 0.0554 | 0.0267 | 1.3715 | 0.0715 | 0.0179 |
| | GELF | 1.1540 | 0.0540 | 0.0268 | 1.3691 | 0.0691 | 0.0181 |
| 75 | SELF | 1.0636 | 0.0363 | 0.0191 | 1.2425 | 0.0574 | 0.0152 |
| | LILF | 1.0617 | 0.0383 | 0.0193 | 1.2411 | 0.0589 | 0.0154 |
| | GELF | 1.0580 | 0.0520 | 0.0195 | 1.2391 | 0.0609 | 0.0155 |
| 100 | SELF | 1.1466 | 0.0466 | 0.0091 | 1.2673 | 0.0326 | 0.0075 |
| | LILF | 1.1460 | 0.0460 | 0.0093 | 1.2659 | 0.0341 | 0.0077 |
| | GELF | 1.1449 | 0.0449 | 0.0094 | 1.2641 | 0.0359 | 0.0079 |

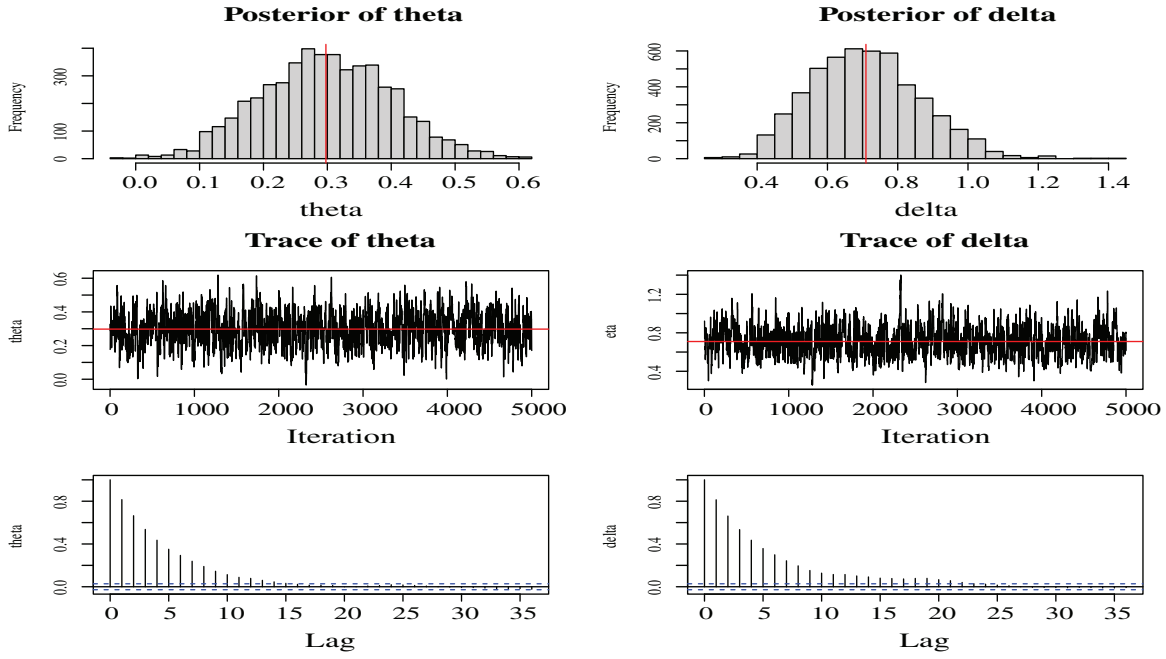


**Figure 3:** MCMC convergence curves of CRED for Table 1

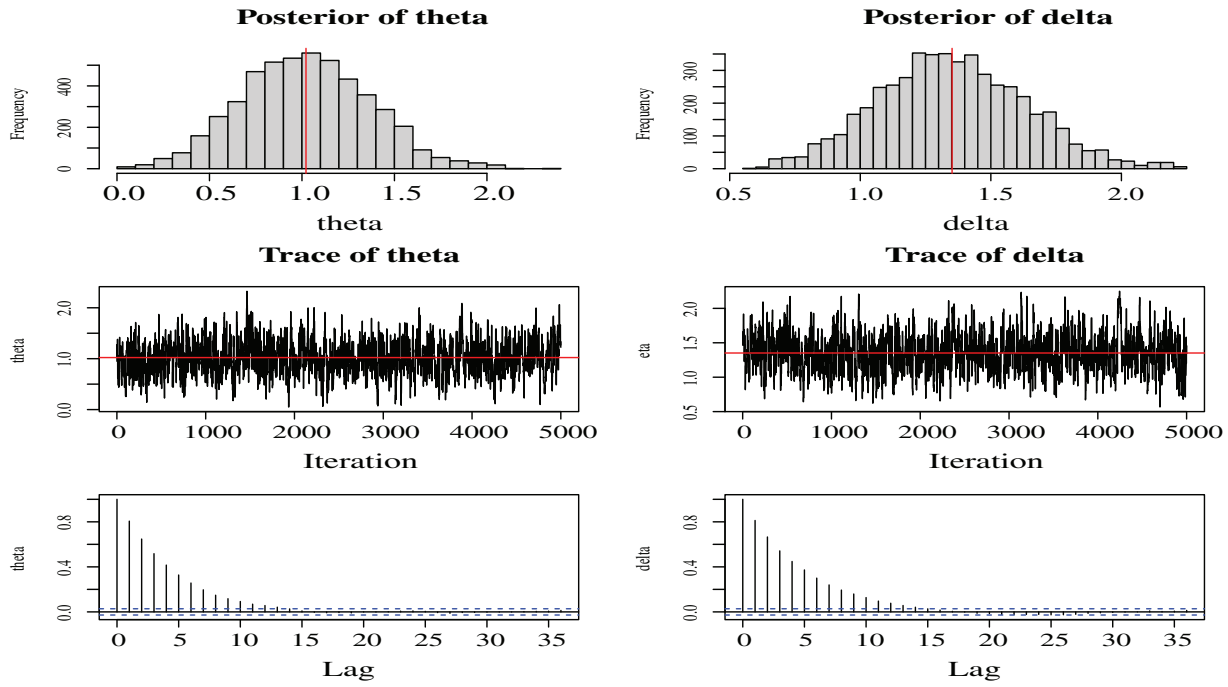


**Figure 4:** MCMC convergence curves of CRED model for Table 3

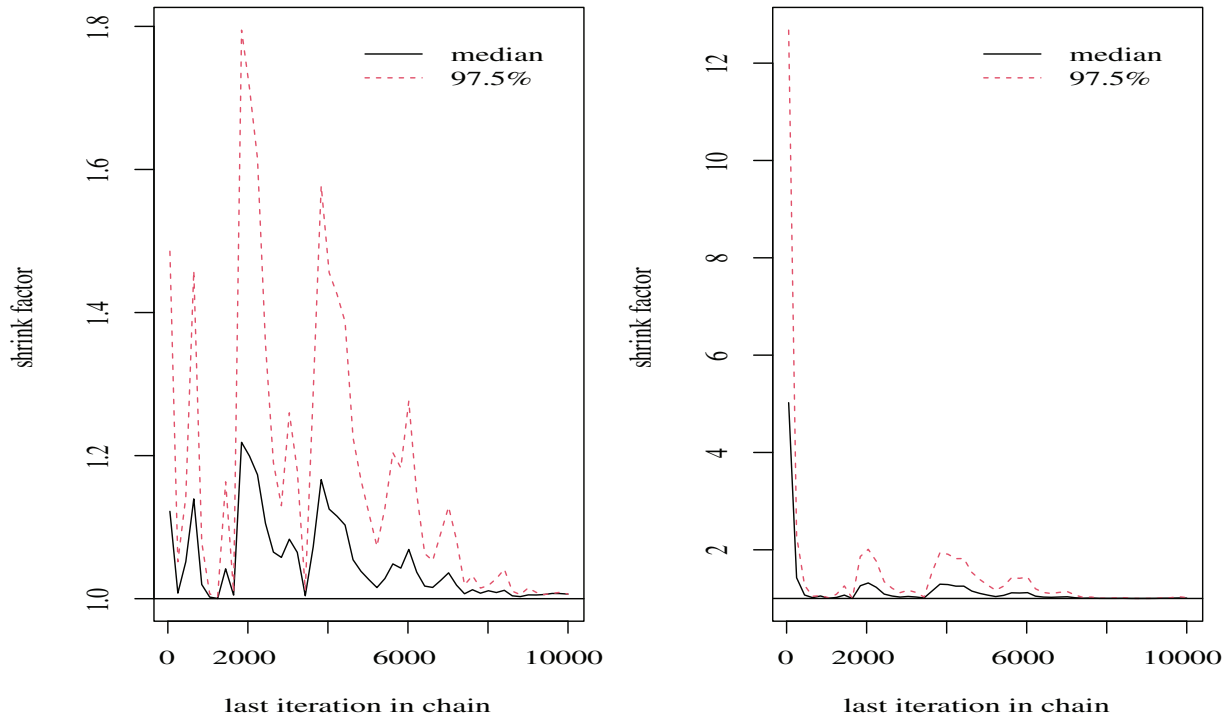


**Figure 5:** (Continued)

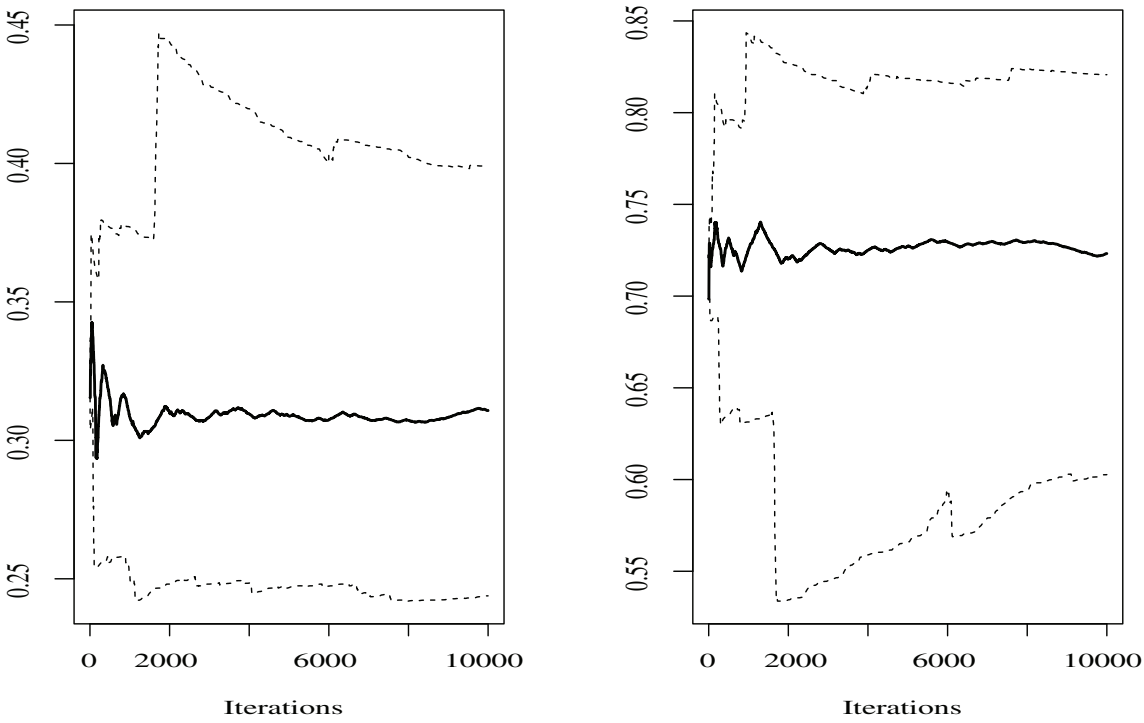


**Figure 5:** Gelman-Rubin curves of $\delta$ and $\eta$ for Table 1

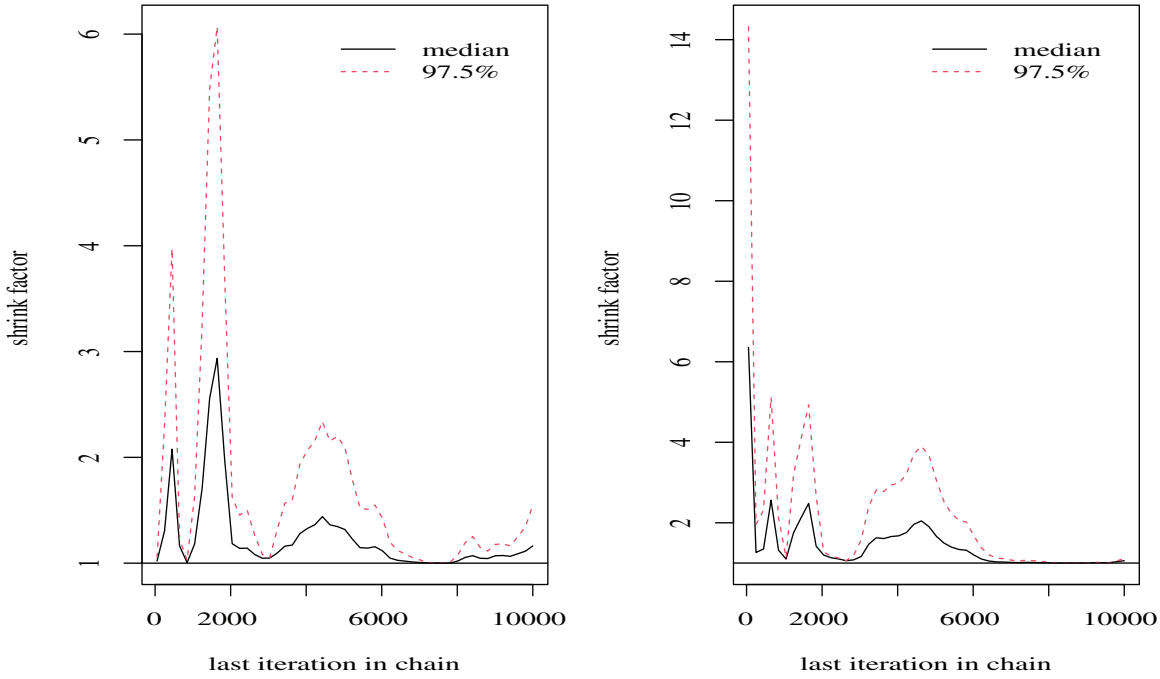


**Figure 6:** (Continued)

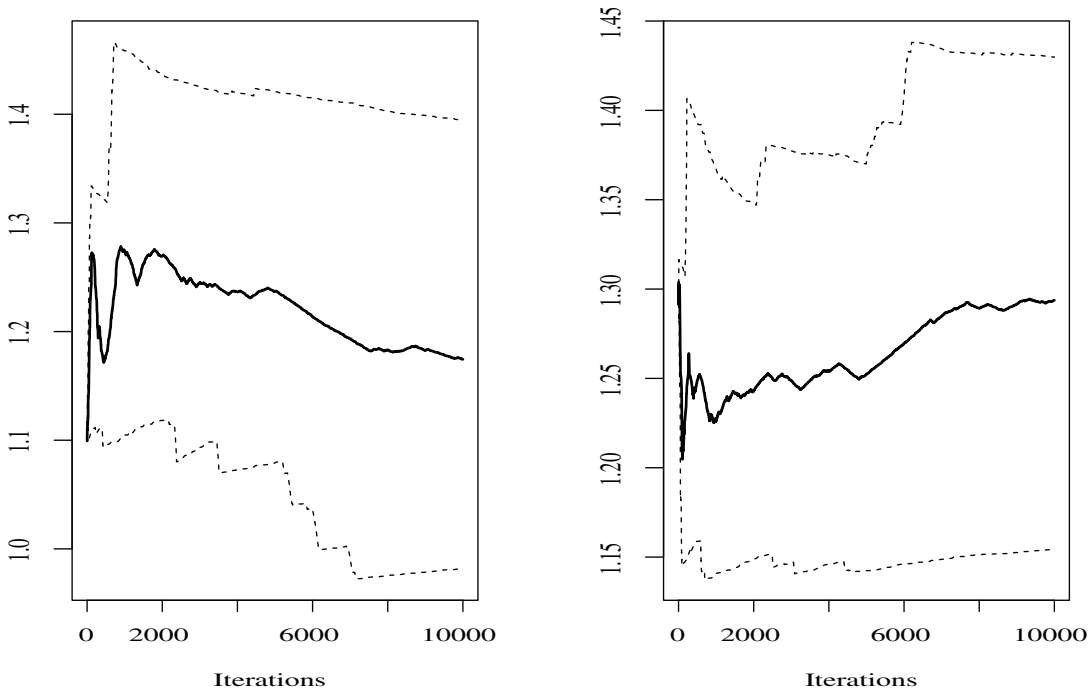


**Figure 6:** Gelman-Rubin curves of $\delta$ and $\eta$ for Table 3

Further, we compute the CIs using the proposed techniques with 95% confidence level. We calculate average interval length (ALs) and coverage probabilities (CPs). The results are presented numerically in Tables 7 and 8. It is well documented that for the informative prior, we choose the values of the parameters in the MH process for the prior distribution as $c_1 = d_1 = c_2 = d_2 = 1$ and the burn-in period $N' = 1000$. Several points can be concluded from these numerical results:

- With increasing $m$, it appears evident that all estimators are generally constant and grow to the initial values of the parameters.
- The MSEs decrease and approach zero in size as $m$ increases. This confirms that the recommended estimators are consistent.
- From the values of MSEs, we observed that the values of MSE of the Bayes method under SELF are less than those of all other methods, which ensures that the Bayes procedure under SELF is superior for estimating the parameter of the CRED among other methods mentioned.
- As the value of $m$ continues to rise, the ALs of $\Xi$ ultimately decrease for all suggested techniques.
- The Boot-t method has greater CPs among approximate, Credible, and Boot-p techniques.

## 4 Actuarial Sciences

Evaluating risk exposures is crucial for businesses in actuarial practice. Forecasting market risks within an instrument portfolio is one of the main duties of actuarial science professionals. In the processes of buying and selling financial products, estimating risk measures is becoming more and more crucial. This section focuses on computing the VaR, TVaR, and TVP for the CRED.

**Table 7:** Numerical Simulation values of CIs under several methods using set 1

| $m$ | | Boot-p | | Boot-t | | Approximate | | Cred Int | |
|---|---|---|---|---|---|---|---|---|---|
| | | AL | CP | AL | CP | AL | CP | AL | CP |
| 25 | $\delta$ | 0.1626 | 0.86 | 0.1337 | 0.94 | 0.3215 | 0.82 | 0.3142 | 0.91 |
| | $\eta$ | 0.0929 | 0.94 | 0.0648 | 0.96 | 0.3703 | 0.9 | 0.3095 | 0.93 |
| 50 | $\delta$ | 0.0894 | 0.87 | 0.0499 | 0.95 | 0.3135 | 0.86 | 0.2689 | 0.86 |
| | $\eta$ | 0.0888 | 0.93 | 0.0634 | 0.97 | 0.3624 | 0.92 | 0.2600 | 0.92 |
| 75 | $\delta$ | 0.0723 | 0.91 | 0.0406 | 0.96 | 0.2569 | 0.90 | 0.2092 | 0.91 |
| | $\eta$ | 0.0763 | 0.95 | 0.0625 | 0.97 | 0.3132 | 0.94 | 0.2045 | 0.93 |
| 100 | $\delta$ | 0.0705 | 0.96 | 0.0402 | 0.98 | 0.2543 | 0.92 | 0.1866 | 0.9 |
| | $\eta$ | 0.0702 | 0.96 | 0.0335 | 0.98 | 0.3016 | 0.95 | 0.1974 | 0.95 |

**Table 8:** Numerical Simulation values of CIs under several methods using set 2

| $m$ | | Boot-p | | Boot-t | | Approximate | | Cred Int | |
|---|---|---|---|---|---|---|---|---|---|
| | | AL | CP | AL | CP | AL | CP | AL | CP |
| 25 | $\delta$ | 0.0931 | 0.88 | 0.0736 | 0.92 | 0.3681 | 0.81 | 0.2669 | 0.84 |
| | $\eta$ | 0.0911 | 0.87 | 0.0770 | 0.93 | 0.3946 | 0.83 | 0.3763 | 0.85 |
| 50 | $\delta$ | 0.0847 | 0.90 | 0.0401 | 0.94 | 0.2970 | 0.86 | 0.2166 | 0.88 |
| | $\eta$ | 0.0859 | 0.91 | 0.0562 | 0.95 | 0.3842 | 0.88 | 0.3119 | 0.91 |
| 75 | $\delta$ | 0.0720 | 0.93 | 0.0352 | 0.97 | 0.2238 | 0.90 | 0.2020 | 0.91 |
| | $\eta$ | 0.0788 | 0.93 | 0.0418 | 0.97 | 0.3780 | 0.91 | 0.2658 | 0.92 |
| 100 | $\delta$ | 0.0706 | 0.96 | 0.0312 | 0.98 | 0.2079 | 0.92 | 0.1849 | 0.94 |
| | $\eta$ | 0.0607 | 0.95 | 0.0337 | 0.98 | 0.1828 | 0.94 | 0.1678 | 0.94 |

### *4.1 VaR Indicator*

One of the most popular metrics for assessing financial risk is the VaR, sometimes referred to as the quantile risk measure or quantile premium principle. At a specific confidence level $p$, usually 90%, 95%, or 99%, it is specified. VaR represents a quantile of the distribution of total losses. Risk managers frequently use VaR to evaluate the possibility of unfavorable outcomes at a given probability level. It aids in assessing risk exposure and calculating the amount of money needed to cover possible

losses. The ability of a company to withstand such extreme events is of particular concern to investors, regulators, and rating agencies. The $p$th quantile of a random variable $W$'s CDF is represented by $\upsilon_1$, and its definition for the CRED is given by

$$\begin{aligned}\upsilon_1 =& G^{-1}(u) \quad ;\sim 0 < u < 1\\ =& \frac{-\eta + \sqrt{4\delta \log(1-u)}}{2\delta}.\end{aligned}$$

### *4.2 TVaR Indicator*

One crucial metric is the TVaR, also known as the conditional tail expectation (CTE). When an event occurs outside of a specific probability level $p$, the expected value of the loss is quantified using the TVaR. The TVaR measure ($\upsilon_2$) for the CRED is determined through the expression below

$$\begin{aligned}\upsilon_2 =& \frac{1}{1-p}\int_{\upsilon_1}^{\infty} wg(w;\delta,\eta)dx\\ =& \frac{1}{1-p}\int_{\upsilon_1}^{\infty} w\,(2\delta w+\eta)\,e^{-\delta w^2-\eta w}\\ =& \frac{1}{1-p}\left\{2\delta\int_{\upsilon_1}^{\infty} w^2\,e^{-\delta w^2-\eta w}\,dw+\eta\int_{\upsilon_1}^{\infty} w\,e^{-\delta w^2-\eta w}\,dw\right\}\\ =& \frac{1}{1-p}\left\{2\delta\sum_{j=0}^{\infty}\frac{(-\delta)^j}{j!}\int_{\upsilon_1}^{\infty} w^{2(j+1)}\,e^{-\eta w}\,dw+\eta\sum_{j=0}^{\infty}\frac{(-\delta)^j}{j!}\int_{\upsilon_1}^{\infty} w^{2j+1}\,e^{-\eta w}\,dw\right\}\\ =& \frac{1}{1-p}\sum_{j=0}^{\infty}\frac{(-\delta)^j}{j!}\left\{2\delta\,\Gamma\left(j+\frac{3}{2},\upsilon_1\eta\right)+\eta\,\Gamma\,(j+2,\upsilon_1\eta)\right\},\end{aligned}$$

where $\Gamma(s,t)=\int_t^{\infty} x^{s-1}e^{-x}dx$ is the upper incomplete gamma function.

### *4.3 TVP Indicator*

Another important metric relevant to insurance science is the Tail Variance Premium (TVP), denoted as ($\upsilon_3$). It provides a more thorough evaluation of risk in the tail of a loss distribution by combining elements of central tendency and dispersion. The TVP of the CRED is expressed mathematically by the following formula:

$$\upsilon_3 = \upsilon_2 + p\,\upsilon_4,$$

where

$$\begin{aligned}\upsilon_4 =& \frac{1}{1-p}\int_{\upsilon_1}^{\infty} w^2 g(w;\delta,\eta)\,dw-(\upsilon_2)^2\\ =& \frac{1}{1-p}\int_{\upsilon_1}^{\infty} w^2\,(2\delta w+\eta)\,e^{-\delta w^2-\eta w}-(\upsilon_2)^2\\ =& \frac{1}{1-p}\left\{2\delta\int_{\upsilon_1}^{\infty} w^3\,e^{-\delta w^2-\eta w}\,dw+\eta\int_{\upsilon_1}^{\infty} w^2\,e^{-\delta w^2-\eta w}\,dw\right\}-(\upsilon_2)^2\end{aligned}$$

$$=\frac{1}{1-p}\sum_{j=0}^{\infty}\frac{(-\delta)^j}{j!}\left\{2\delta\,\Gamma\,(j+2,\upsilon_1\eta)+\eta\,\Gamma\left(j+\frac{3}{2},\upsilon_1\eta\right)\right\}-(\upsilon_2)^2.$$

### *4.4 Numerical Simulation Analysis for the Actuarial Sciences*

In this part of the study, we apply our the CRED and RD with two scenarios of unknown parameters $\delta$ and $\eta$ to provide a number of results for the measures $\upsilon_1$, $\upsilon_2$, and $\upsilon_3$. Tables 9 and 10 present a summary and report of the findings. From now on, Figs. 7 and 8 present a graphic plot of the comparisons between the two distributions. With higher values of $\upsilon_1$, $\upsilon_2$, and $\upsilon_3$ than the RD, the CRED can be regarded as heavier among the RD based on these figures. As a result, modeling heavy-tailed data sets is better suited for the CRED.

**Table 9:** Numerical Simulation records of $\upsilon_1$, $\upsilon_2$, and $\upsilon_3$ for CRED and RD

| Model | Parameter | $p$ | $\upsilon_1$ | $\upsilon_2$ | $\upsilon_3$ |
|---|---|---|---|---|---|
| CRED | $\delta=0.3,\ \eta=2.2$ | 0.65 | 0.4496 | 0.8228 | 0.9016 |
| | | 0.75 | 0.5836 | 0.9467 | 1.0332 |
| | | 0.85 | 0.7794 | 1.1285 | 1.2200 |
| | | 0.95 | 1.1738 | 1.4975 | 1.5869 |
| | | 0.99 | 1.6994 | 1.9945 | 2.0731 |
| RD | $\delta=0.3$ | 0.65 | 0.4347 | 0.5929 | 0.6042 |
| | | 0.75 | 0.4995 | 0.6437 | 0.6550 |
| | | 0.85 | 0.5843 | 0.7132 | 0.7240 |
| | | 0.95 | 0.7343 | 0.8424 | 0.8514 |
| | | 0.99 | 0.9104 | 1.0009 | 1.0079 |

**Table 10:** Numerical Simulation records of $\upsilon_1$, $\upsilon_2$, and $\upsilon_3$ for CRED and RD

| Model | Parameter | $p$ | $\upsilon_1$ | $\upsilon_2$ | $\upsilon_3$ |
|---|---|---|---|---|---|
| CRED | $\delta=0.75,\ \eta=0.1$ | 0.65 | 1.1183 | 1.5486 | 1.6320 |
| | | 0.75 | 1.2945 | 1.6867 | 1.7705 |
| | | 0.85 | 1.5251 | 1.8758 | 1.9557 |
| | | 0.95 | 1.9330 | 2.2271 | 2.2942 |
| | | 0.99 | 2.4121 | 2.6583 | 2.7100 |
| RD | $\delta=0.75$ | 0.65 | 1.0867 | 1.4824 | 1.5529 |
| | | 0.75 | 1.2488 | 1.6093 | 1.6802 |
| | | 0.85 | 1.4609 | 1.7831 | 1.8507 |
| | | 0.95 | 1.8358 | 2.1060 | 2.1627 |
| | | 0.99 | 2.2761 | 2.5023 | 2.5459 |

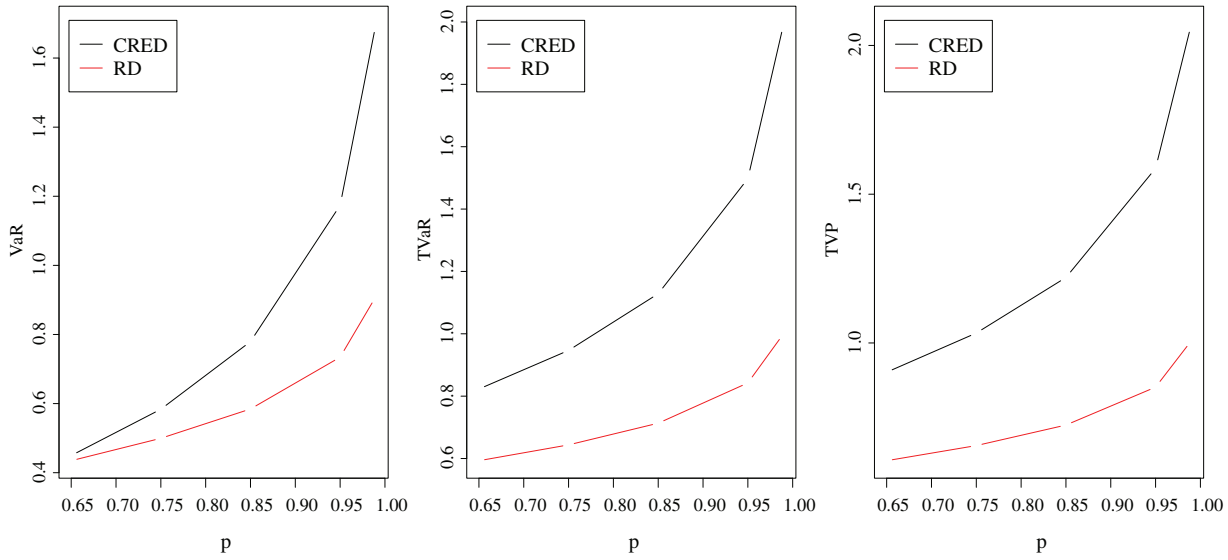


**Figure 7:** Graphical plots of computational value of $\upsilon_1$, $\upsilon_2$, and $\upsilon_3$ in Table 9

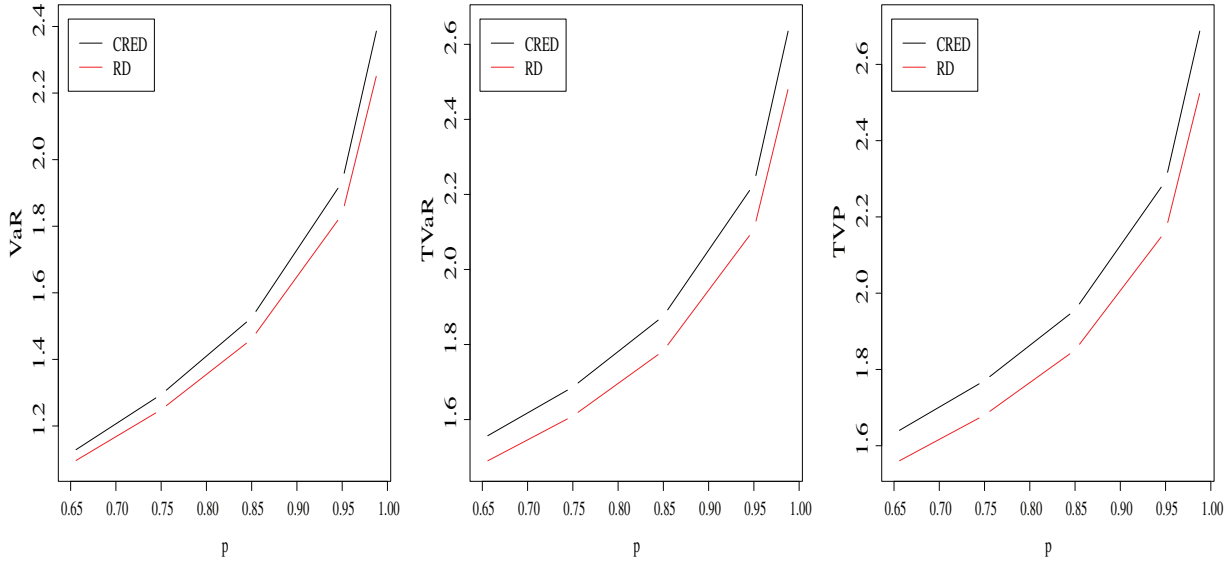


**Figure 8:** Graphical plots of computational value of $\upsilon_1$, $\upsilon_2$, and $\upsilon_3$ in Table 10

## 5 Application to Real Data Sets

This section demonstrates the practical utility of the proposed model using two distinct real-world data sets. The results highlight the advantages of the CRED model and its strong compatibility with the analyzed data sets.

### *5.1 Data Set I*

This data set considered the survival times of 121 patients with breast cancer between 1929 and 1938. These values were taken from a large hospital and studied by Yusra et al. [52]. Table 11 summarizes the values of the survival times of patients.

**Table 11:** The survival times of patients

| | | | | | | | | | |
|---|---|---|---|---|---|---|---|---|---|
| 0.3 | 0.3 | 4.0 | 5.0 | 5.6 | 6.2 | 6.3 | 6.6 | 6.8 | 7.4 |
| 7.5 | 8.4 | 8.4 | 10.3 | 11.0 | 11.8 | 12.2 | 12.3 | 13.5 | 14.4 |
| 14.4 | 14.8 | 15.5 | 15.7 | 16.2 | 16.3 | 16.5 | 16.8 | 17.2 | 17.3 |
| 17.5 | 17.9 | 19.8 | 20.4 | 20.9 | 21.0 | 21.0 | 21.1 | 23.0 | 23.4 |
| 23.6 | 24.0 | 24.0 | 27.9 | 28.2 | 29.1 | 30.0 | 31.0 | 31.0 | 32.0 |
| 35.0 | 35.0 | 37.0 | 37.0 | 37.0 | 38.0 | 38.0 | 38.0 | 39.0 | 39.0 |
| 40.0 | 40.0 | 40.0 | 41.0 | 41.0 | 41.0 | 42.0 | 43.0 | 43.0 | 43.0 |
| 44.0 | 45.0 | 45.0 | 46.0 | 46.0 | 47.0 | 48.0 | 49.0 | 51.0 | 51.0 |
| 51.0 | 52.0 | 54.0 | 55.0 | 56.0 | 57.0 | 58.0 | 59.0 | 60.0 | 60.0 |
| 60.0 | 61.0 | 62.0 | 65.0 | 65.0 | 67.0 | 67.0 | 68.0 | 69.0 | 78.0 |
| 80.0 | 83.0 | 88.0 | 89.0 | 90.0 | 93.0 | 96.0 | 103.0 | 105.0 | 109.0 |
| 109.0 | 111.0 | 115.0 | 117.0 | 125.0 | 126.0 | 127.0 | 129.0 | 129.0 | 139.0 |
| 154.0 | | | | | | | | | |

### *5.2 Data Set II*

Here, we applied the quarterly evolution of the number of foreign licenses in the construction area in Saudi Arabia. The values of the data sets are taken from https://datasaudi.sa/en/sector/construction#real-sector-indicators (accessed on 27 October 2025), as well as it was used by Badr et al. [53]. Table 12 summarized the considered values.

**Table 12:** The quarterly evolution of the number of foreign licenses in Saudi Arabia

| | | | | | | | |
|---|---|---|---|---|---|---|---|
| 8 | 6 | 8 | 16 | 23 | 20 | 28 | 40 |
| 43 | 50 | 54 | 32 | 52 | 29 | 33 | 42 |
| 41 | 52 | 56 | 79 | 155 | 84 | 95 | 111 |
| 136 | | | | | | | |

### *5.3 Data Set III*

According to Arshad et al. [54], the fatigue fracture of Kevlar 373/epoxy under continuous pressure at 90% stress level until everything failed can be explained by the following moderate data set. The findings of the proposed data sets are tabulated in Table 13.

### *5.4 Data Set VI*

The percentage of 75 countries' primary energy consumption in 2019 was determined by this dataset. The proposed data comes from renewable technology, which has been previously examined by Eslam et al. [55]. Table 14 revealed the suggested data's values.

It is well documented that we divided the values of the first and second data sets by 10 for computational purposes. Furthermore, to investigate potential outliers, Figs. 9–12 plotted numerous non-parametric curves, including the kernel density, total test time (TTT), probability-probability (PP) plot, QQ plot, the histogram, and box plot.

Several existing distributions that are used to compare their suitability and flexibility with the newly CRED. The competing distributions are Nadarajah Haghighi (NH), Compound exponential Xlindley (CEXL), zero-truncated Poisson-Lindley (ZTP-Lind), exponential, and Rayleigh distributions. The choice of optimal performance associated with the fitting models is determined through targeted evaluation metrics, including the Akaike Information Criterion ($\mathcal{F}_1$), the Bayesian Information Criterion ($\mathcal{F}_2$), Kolmogorov-Smirnov ($\mathcal{KS}$) statistics, and its associated $p$-values. In general, a model with the lowest statistical metrics and the highest $p$-values chosen the best fitting model for the associated data set.

**Table 13:** Fatigue fracture of Kevlar 373/epoxy data set

| | | | | | | | | | |
|---|---|---|---|---|---|---|---|---|---|
| 0.0251 | 0.0886 | 0.0891 | 0.2501 | 0.3113 | 0.3451 | 0.4763 | 0.5650 | 0.5671 | 0.6566 |
| 0.6748 | 0.6751 | 0.6753 | 0.7696 | 0.8375 | 0.8391 | 0.8425 | 0.8645 | 0.8851 | 0.9113 |
| 0.9120 | 0.9836 | 1.0483 | 1.0596 | 1.0773 | 1.1733 | 1.2570 | 1.2766 | 1.2985 | 1.3211 |
| 1.3503 | 1.3551 | 1.4595 | 1.4880 | 1.5728 | 1.5733 | 1.7083 | 1.7263 | 1.7460 | 1.7630 |
| 1.7746 | 1.8275 | 1.8375 | 1.8503 | 1.8808 | 1.8878 | 1.8881 | 1.9316 | 1.9558 | 2.0048 |
| 2.0408 | 2.0903 | 2.1093 | 2.1330 | 2.2100 | 2.2460 | 2.2878 | 2.3203 | 2.3470 | 2.3513 |
| 2.4951 | 2.5260 | 2.9911 | 3.0256 | 3.2678 | 3.4045 | 3.4846 | 3.7433 | 3.7455 | 3.9143 |
| 4.8073 | 5.4005 | 5.4435 | 5.5295 | 6.5541 | 9.0960 | | | | |

**Table 14:** Renewable technology data set

| | | | | | | | | | |
|---|---|---|---|---|---|---|---|---|---|
| 0.310 | 6.618 | 0.402 | 0.799 | 0.618 | 0.325 | 0.064 | 2.285 | 6.540 | 0.2539 |
| 1.064 | 0.618 | 0.871 | 0.213 | 0.518 | 0.920 | 1.266 | 7.908 | 1.629 | 1.410 |
| 0.077 | 0.251 | 1.649 | 3.016 | 2.499 | 0.056 | 3.064 | 2.615 | 3.039 | 0.694 |
| 9.310 | 0.730 | 0.888 | 0.456 | 0.254 | 0.311 | 1.445 | 0.248 | 0.609 | 4.502 |
| 3.540 | 5.870 | 1.092 | 1.356 | 1.697 | 0.709 | 0.778 | 0.221 | 0.406 | 1.071 |
| 0.027 | 2.445 | 7.220 | 1.590 | 2.154 | 1.173 | 0.393 | 0.230 | 4.224 | 0.101 |
| 0.834 | 1.522 | 1.818 | 12.11 | 1.847 | 1.748 | 1.405 | 2.733 | 3.370 | 1.545 |
| 0.601 | 0.857 | 1.054 | 2.764 | 15.74 | | | | | |

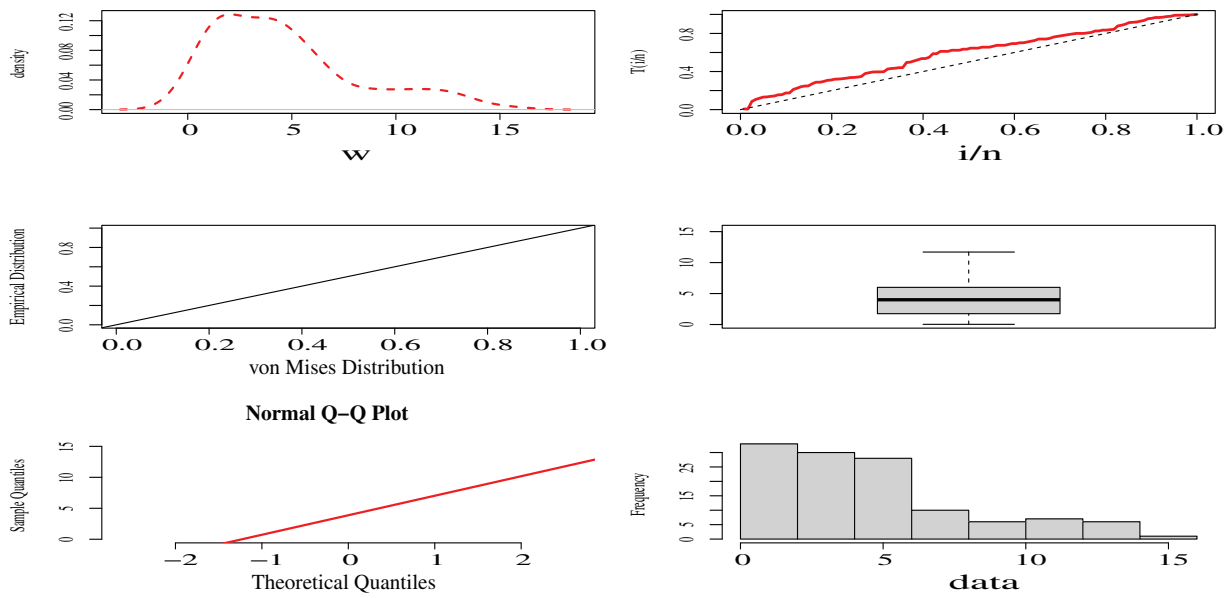


**Figure 9:** Numerous non-parametric plots of data set I

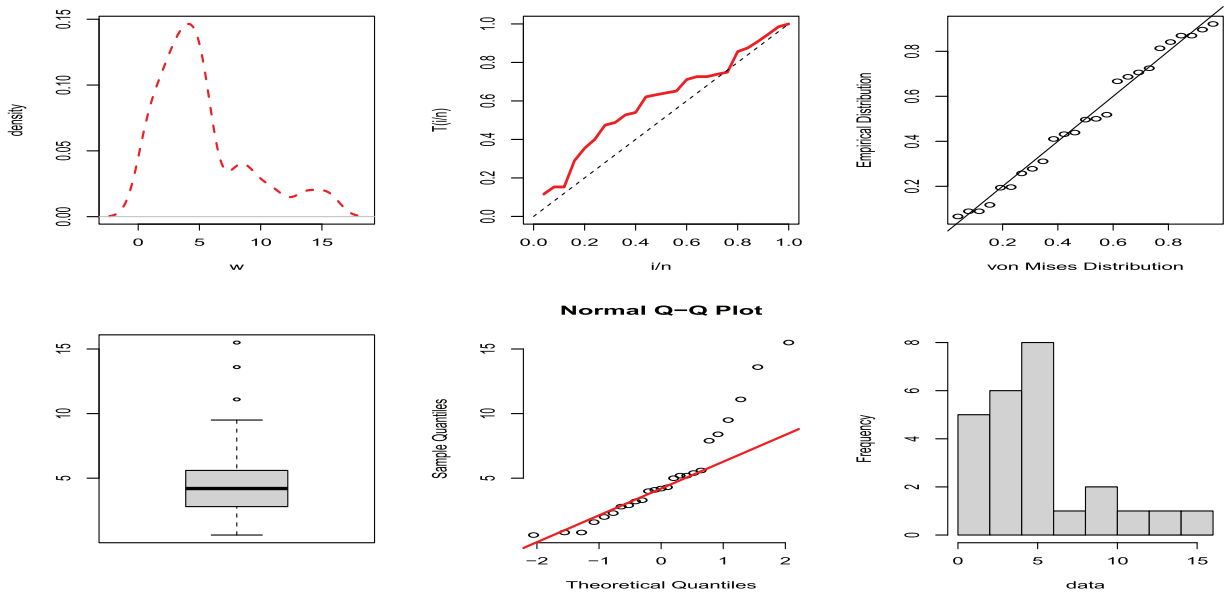


**Figure 10:** Numerous non-parametric plots of data set II

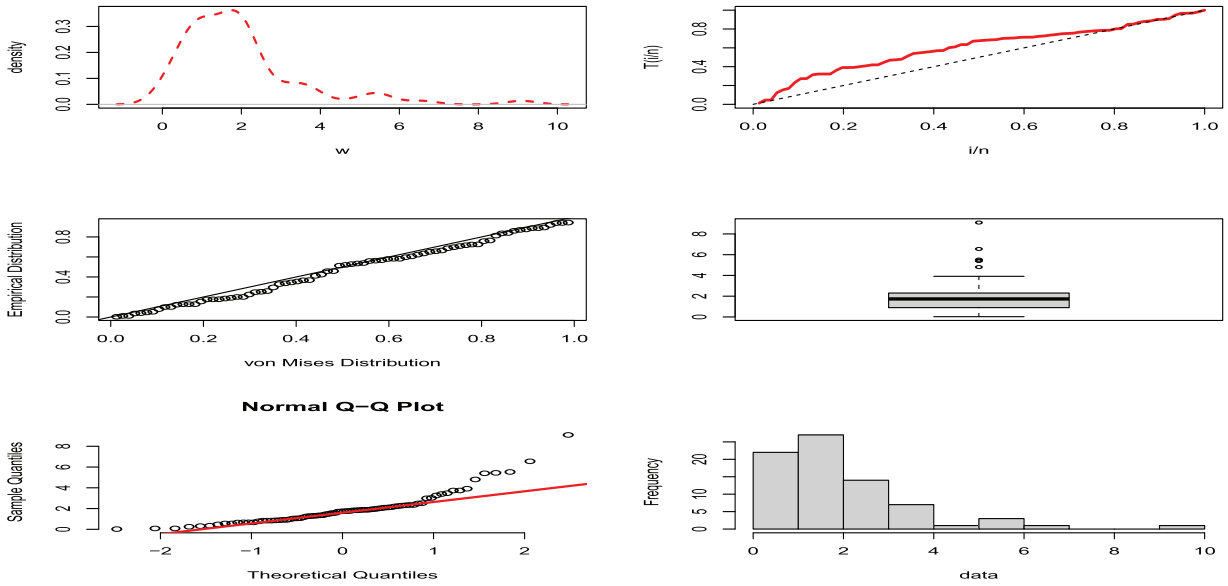


**Figure 11:** Numerous non-parametric plots of data set III

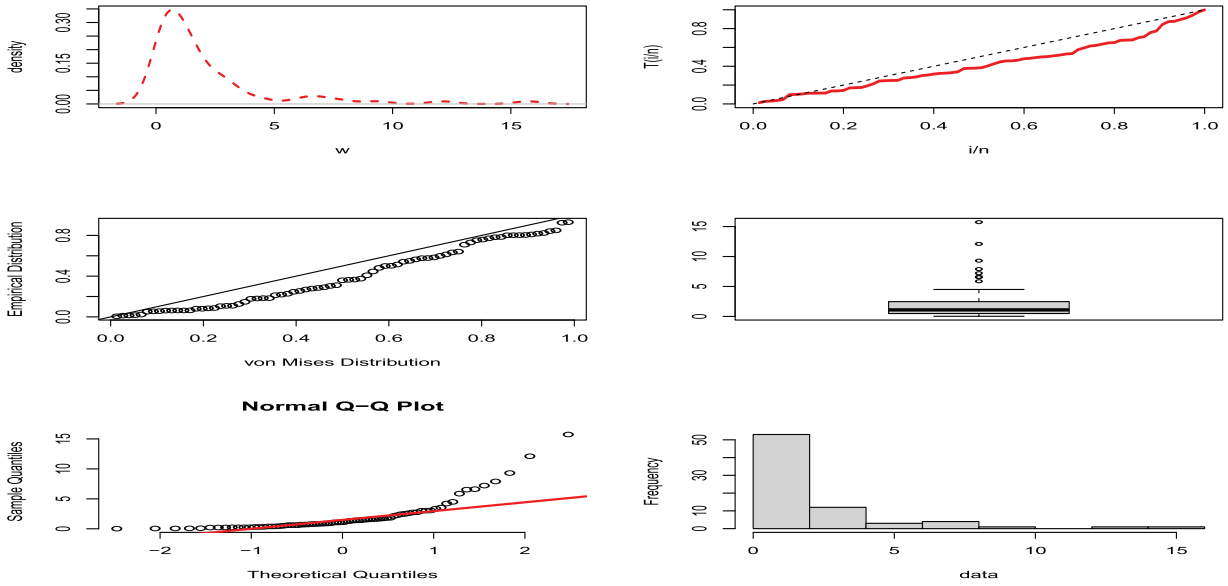


**Figure 12:** Numerous non-parametric plots of data set VI

The results of the numerical values obtained are recorded in Table 15. According to these results, the CRED is the most suitable candidate for modeling the four proposed data sets. In addition, Figs. 13–20 show empirical PDF, CDF, and PP plots for the fitting distribution using the recommended data sets, which also supports our findings that the CRED performs better than the other competing distributions as well as a close fit to the data sets.

**Table 15:** The estimated parameters and the goodness-of-fit statistics for the four data sets

| Data set | Dist | $\hat{\delta}$ | $\hat{\eta}$ | $\mathcal{F}_1$ | $\mathcal{F}_2$ | $\mathcal{KS}$ | $\mathcal{P}$-value |
|---|---|---|---|---|---|---|---|
| I | CRED | 0.0116 | 0.1308 | 605.384 | 610.976 | 0.0526 | 0.8907 |
| | CEXL | 0.4020 | 0.0598 | 606.799 | 612.391 | 0.0748 | 0.5065 |
| | NH | 2.1031 | 0.0785 | 606.917 | 612.509 | 0.0788 | 0.4397 |
| | ZTP-Lind | 0.4663 | 1.3265 | 607.012 | 612.604 | 0.0824 | 0.3832 |
| | Exp | | 0.2158 | 615.029 | 617.825 | 0.1203 | 0.0600 |
| | Rayleigh | | 4.1109 | 646.754 | 649.550 | 0.1986 | 0.0001 |
| II | CRED | 0.0089 | 0.1282 | 133.232 | 135.670 | 0.1278 | 0.8081 |
| | CEXL | 1.0021 | 0.6711 | 133.484 | 135.922 | 0.0559 | 0.7433 |
| | NH | 1.5756 | 0.1032 | 134.266 | 136.704 | 0.1484 | 0.6401 |
| | ZTP-Lind | 0.5578 | 3.6661 | 136.486 | 138.923 | 0.1541 | 0.5927 |
| | Exp | | 0.1933 | 134.163 | 135.381 | 0.1781 | 0.4060 |
| | Rayleigh | | 4.5421 | 135.912 | 137.131 | 0.2276 | 0.1497 |
| III | CRED | 0.0564 | 0.3294 | 252.972 | 257.634 | 0.1268 | 0.1587 |
| | CEXL | 0.9029 | 0.2136 | 254.929 | 259.590 | 0.1414 | 0.0864 |
| | NH | 1.6828 | 0.2462 | 253.695 | 258.357 | 0.1309 | 0.1347 |
| | ZTP-Lind | 1.5036 | 4.9757 | 264.643 | 269.305 | 0.1406 | 0.0897 |
| | Exp | | 0.5105 | 256.228 | 258.559 | 0.1663 | 0.0262 |
| | Rayleigh | | 1.7723 | 276.639 | 278.970 | 0.2042 | 0.0029 |
| VI | CRED | 0.0128 | 0.5528 | 260.504 | 265.139 | 0.0830 | 0.6794 |
| | CEXL | 26.675 | 26.165 | 264.657 | 269.292 | 0.1212 | 0.2199 |
| | NH | 0.4745 | 2.1684 | 261.582 | 266.217 | 0.1181 | 0.2463 |
| | ZTP-Lind | 0.5383 | 1.8334 | 263.957 | 268.592 | 0.0976 | 0.4713 |
| | Exp | | 0.4790 | 262.421 | 264.738 | 0.1195 | 0.2345 |
| | Rayleigh | | 2.4506 | 415.129 | 417.446 | 0.4594 | $< 0.0001$ |

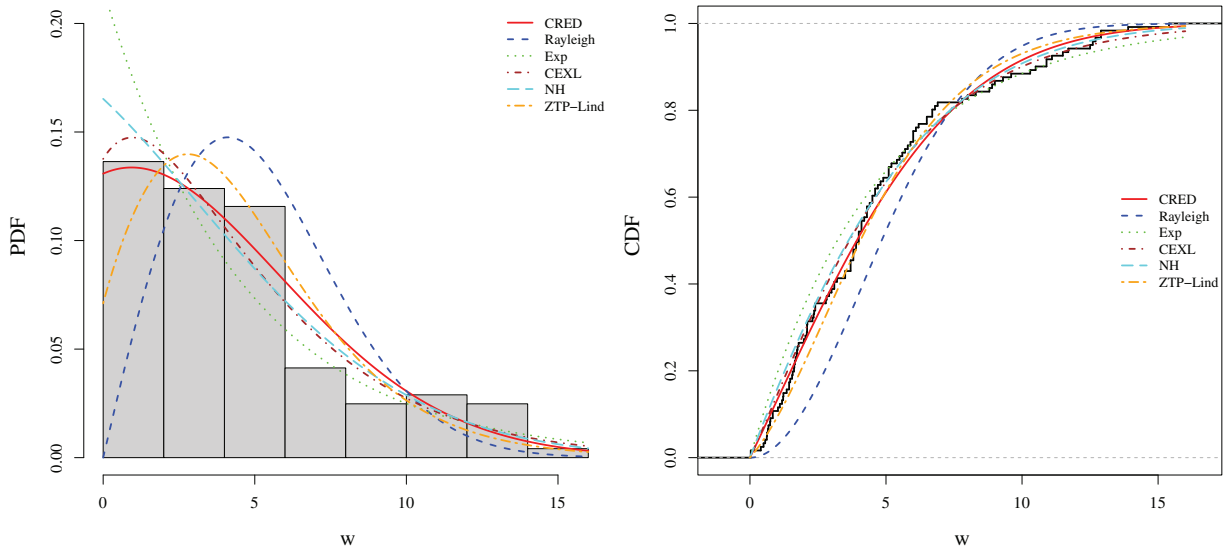


**Figure 13:** The PDFs and CDFs plots of the fitted distributions for Data I

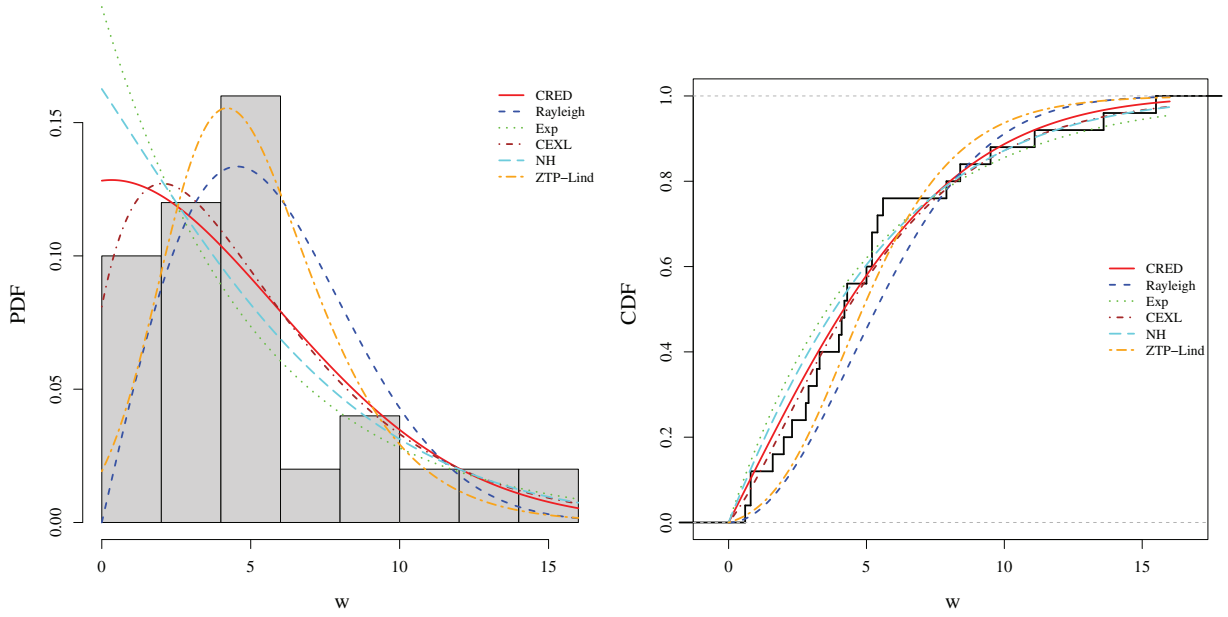


**Figure 14:** The PDFs and CDFs plots of the fitted distributions for Data II

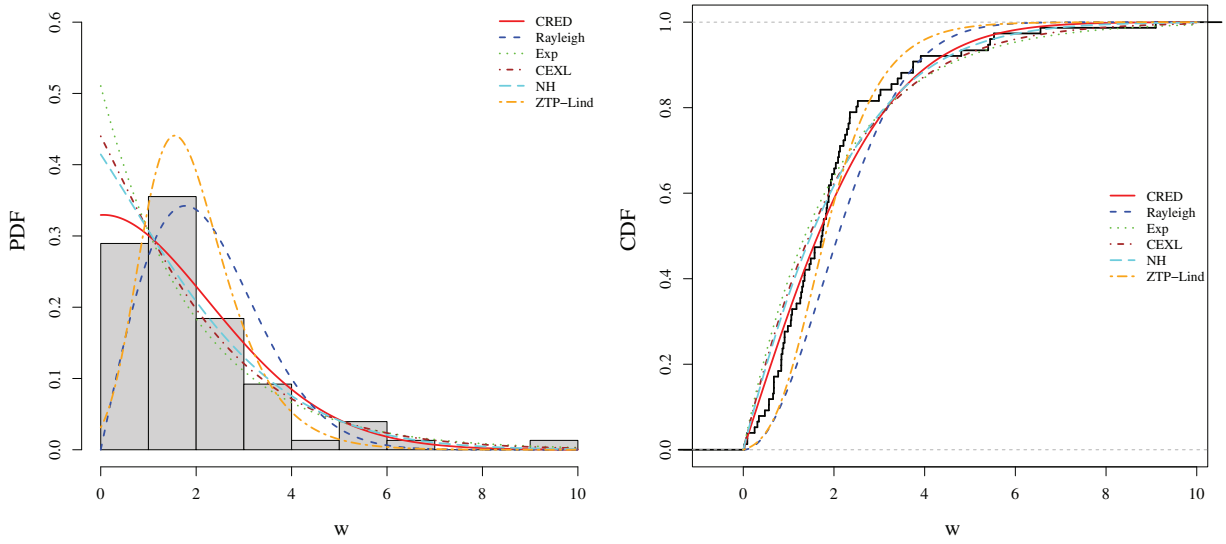


**Figure 15:** The PDFs and CDFs plots of the fitted distributions for Data III

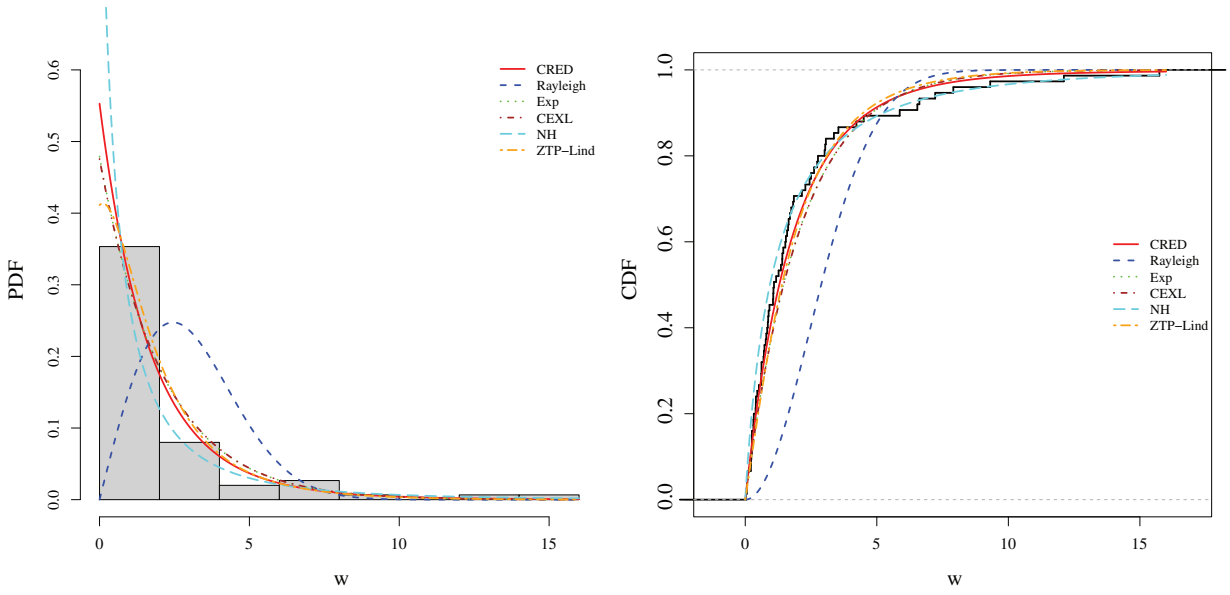


**Figure 16:** The PDFs and CDFs plots of the fitted distributions for Data VI

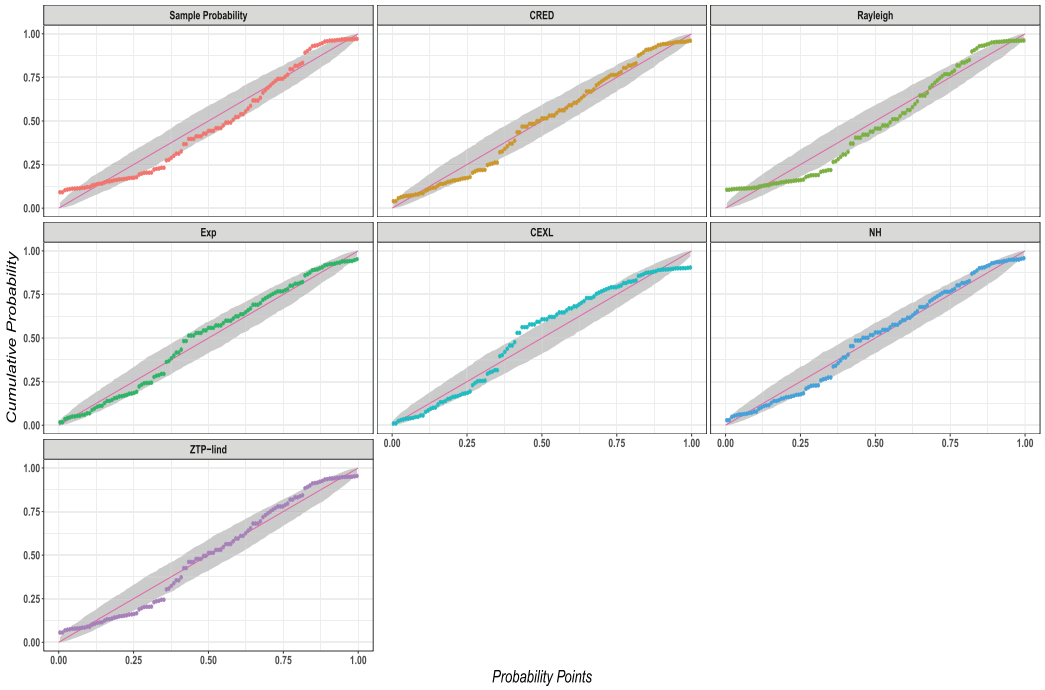


**Figure 17:** P-P plots for data I

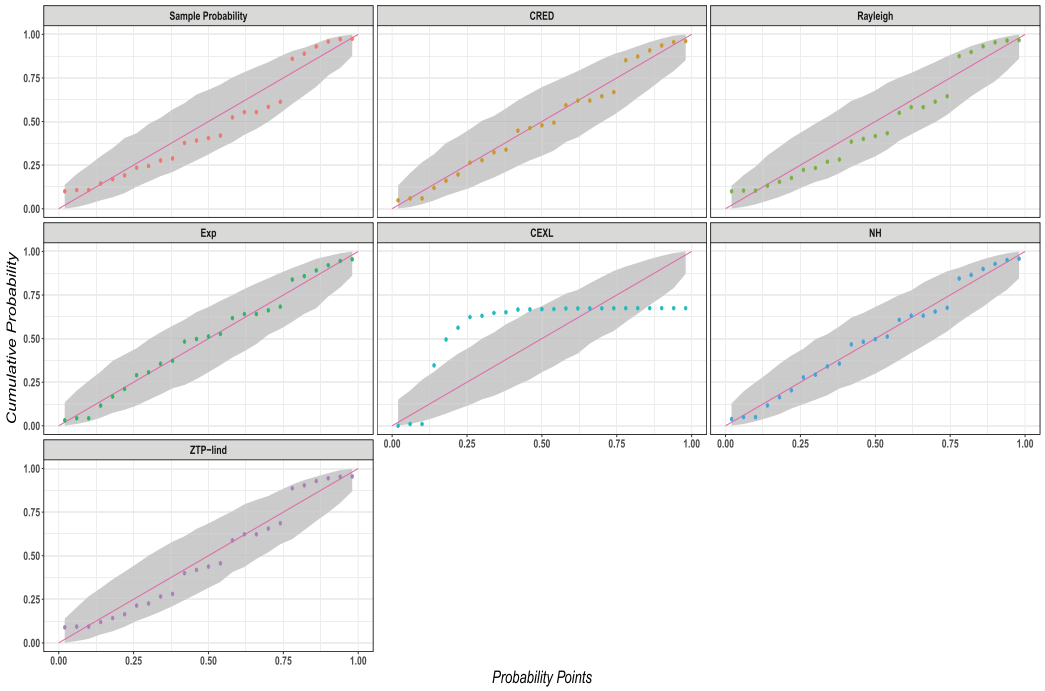


**Figure 18:** P-P plots for data II

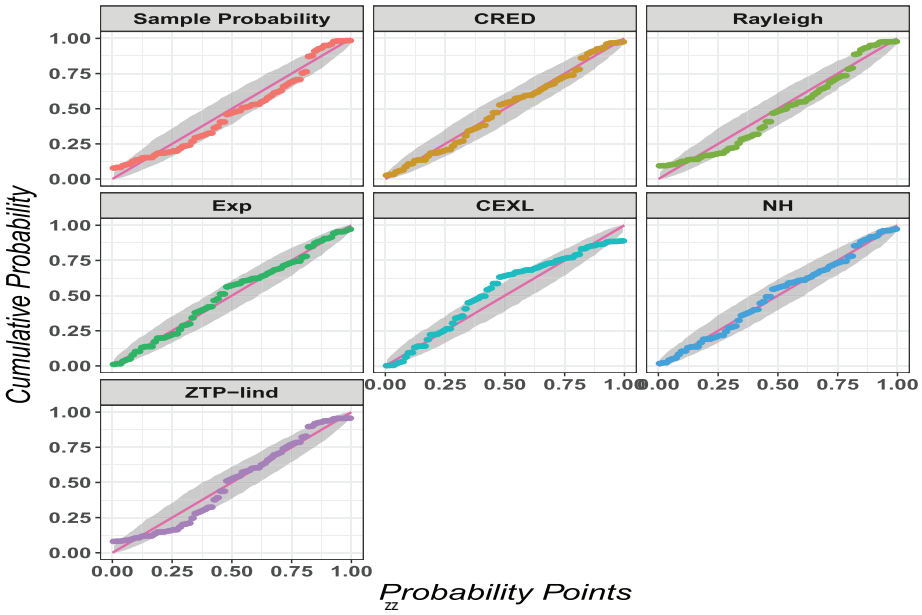


**Figure 19:** P-P plots for data III

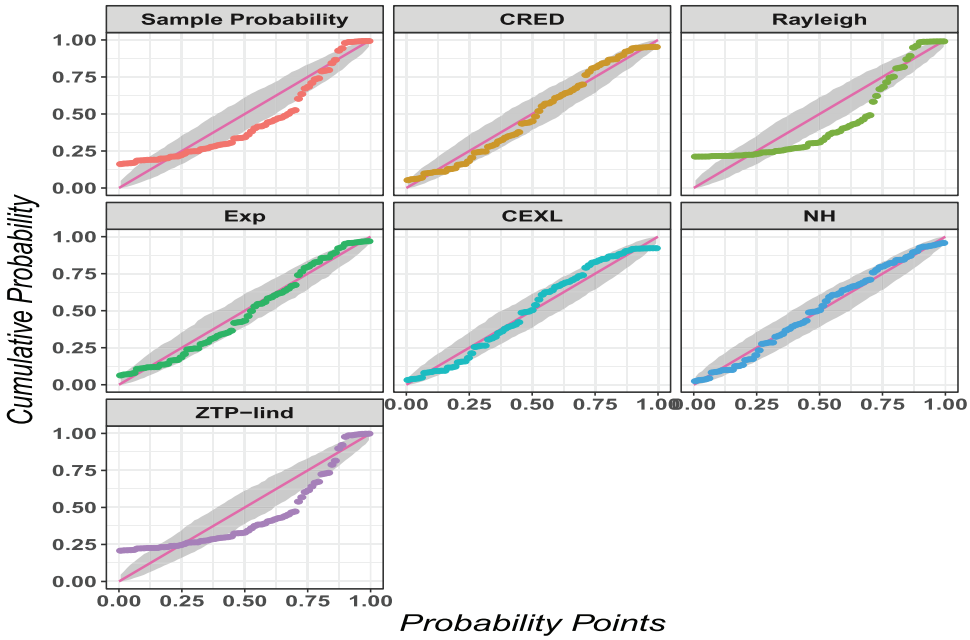


**Figure 20:** P-P plots for data VI

In the end, the results of the classical and Bayesian estimation based on the proposed loss functions considering the four data sets are summarized in Table 16. Furthermore, for the MCMC convergence and by applying the suggested data sets, Figs. 21–24 plotted the histogram, trace, and ACF plots of the CRED for the two parameters $\delta$ and $\eta$.

**Table 16:** Bayesian and non-Bayesian estimators results of the CRED

| Data | | $\mathcal{S}_2$ | $\mathcal{S}_3$ | $\mathcal{S}_4$ | $\mathcal{S}_5$ | $\mathcal{S}_6$ | SELF | LILF | GELF |
|---|---|---|---|---|---|---|---|---|---|
| I | $\delta$ | 0.0121 | 0.0134 | 0.0123 | 0.0143 | 0.0115 | 0.0116 | 0.0114 | 0.0117 |
| | $\eta$ | 0.1357 | 0.1291 | 0.1298 | 0.1253 | 0.1332 | 0.1323 | 0.1321 | 0.1322 |
| II | $\delta$ | 0.0077 | 0.0151 | 0.0115 | 0.0203 | 0.0121 | 0.0091 | 0.0093 | 0.0093 |
| | $\eta$ | 0.1389 | 0.0956 | 0.1073 | 0.0737 | 0.1026 | 0.1283 | 0.1285 | 0.1287 |
| III | $\delta$ | 0.0551 | 0.0557 | 0.0563 | 0.0367 | 0.0577 | 0.0511 | 0.0513 | 0.0518 |
| | $\eta$ | 0.3202 | 0.3249 | 0.3242 | 0.3214 | 0.3271 | 0.3282 | 0.3286 | 0.3288 |
| VI | $\delta$ | 0.0149 | 0.0174 | 0.0201 | 0.0212 | 0.0184 | 0.0135 | 0.0138 | 0.0139 |
| | $\eta$ | 0.5519 | 0.5523 | 0.5617 | 0.5648 | 0.5563 | 0.5542 | 0.5544 | 0.5549 |

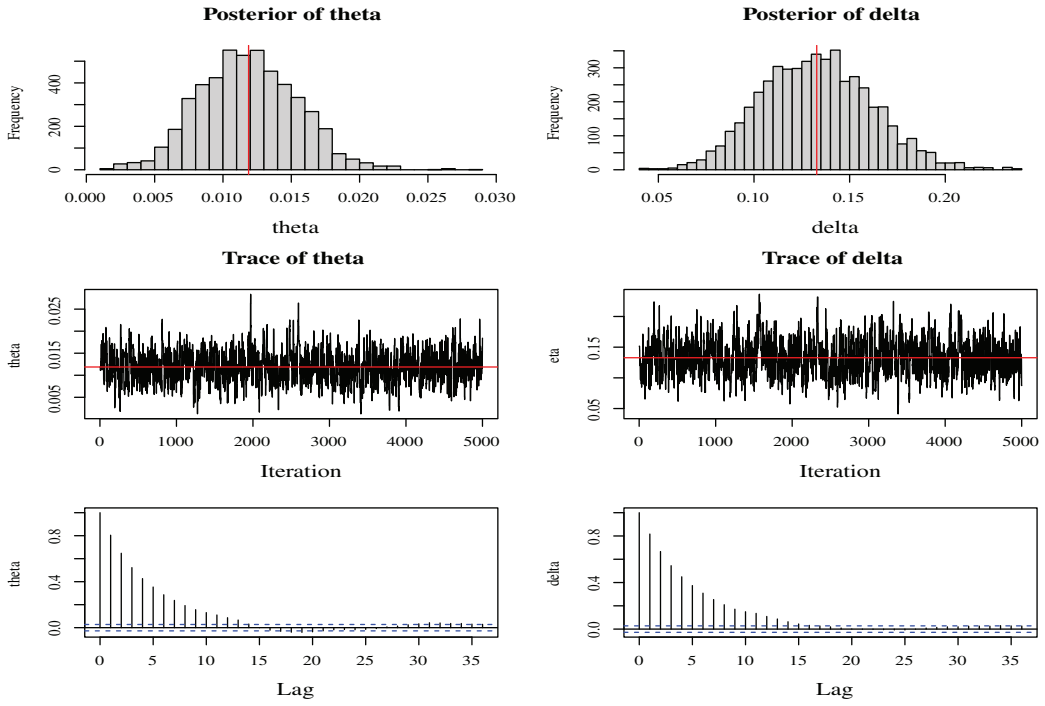


**Figure 21:** MCMC convergence results for data I

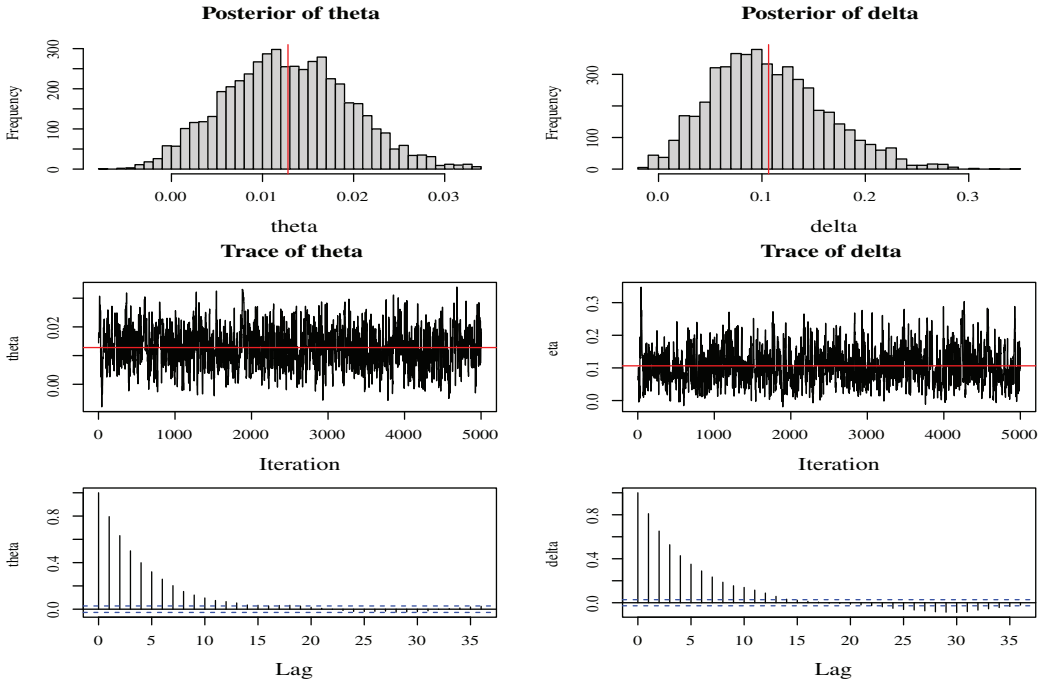


**Figure 22:** MCMC convergence results for data II

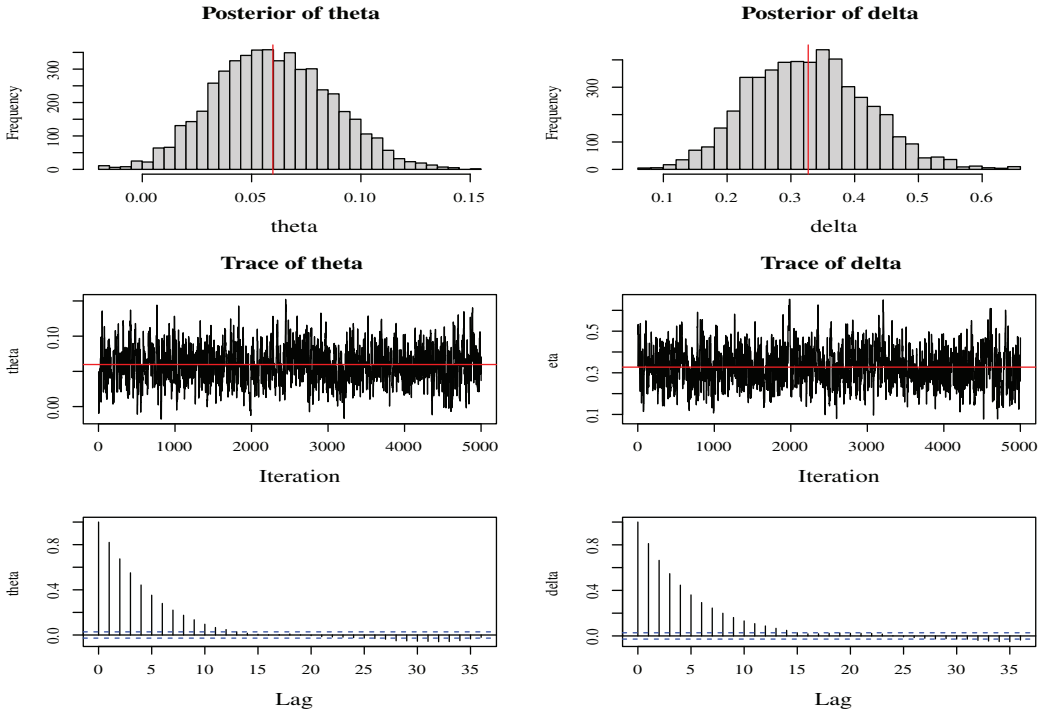


**Figure 23:** MCMC convergence results for data III

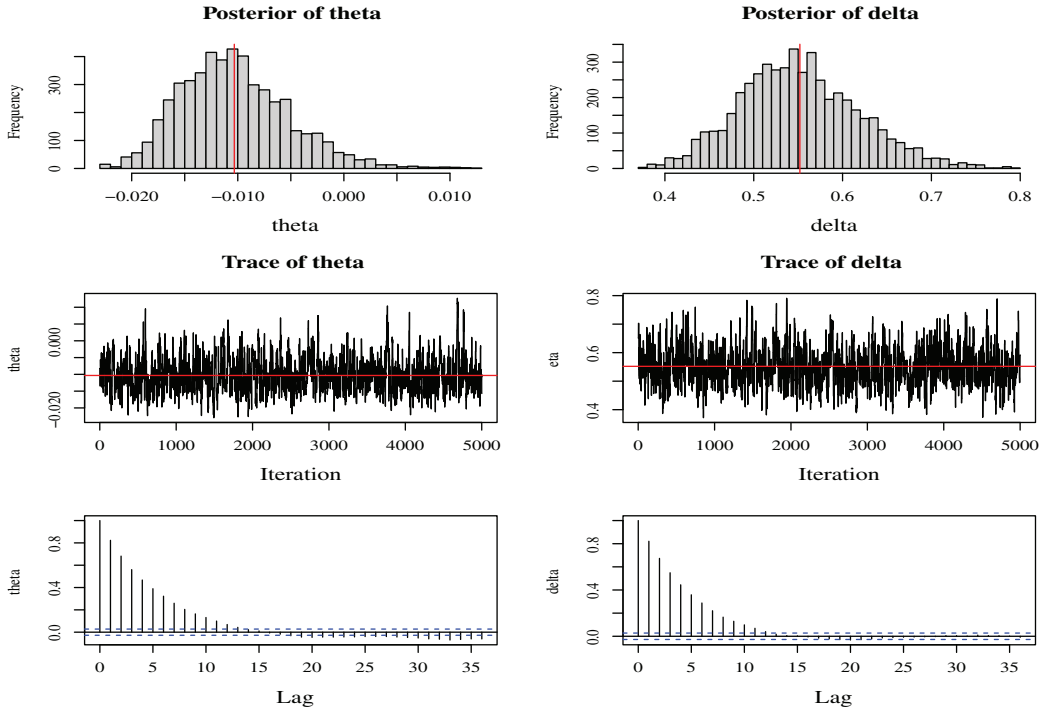


**Figure 24:** MCMC convergence results for data VI

## 6 Conclusion

In this study, we investigate several Bayesian and non-Bayesian estimators to identify the most efficient estimators for the unknown parameters of the CRED. The simulation study clearly indicates that the Bayes approach under SELF is superior to the conventional estimating method since it consistently produces lower values for the MSE. Thus, to sum up, we can say that Bayes estimators based on SELE for the two parameters $\delta$ and $\eta$ are the most efficient estimators. We also discussed actuarial measures such as VaR, TVaR, and TVP, which highlight the usefulness of the CRED in both reliability and risk management contexts. In the end, four applications were taken from different fields to demonstrate the applicability of the CRED, and it is shown that it is more efficiently analyzed in all proposed data sets. The proposed CRED model can be applied to other data sets, such as bi-modal, symmetrical, and asymmetrical data for further research studies. Another future work is to estimate the model parameters in censoring types (type I, type II, and hybrid process). In addition to best-fitting capability, the CRED has certain disadvantages. The CRED has a non-closed form for the associated moment and related measures. Also, it is not appropriate to analyze the discrete data sets.

**Acknowledgement:** Not applicable.

**Funding Statement:** The authors received no specific funding for this study

**Author Contributions:** The authors confirm contribution to the paper as follows: Ibrahim Hassan Alkhairy and Hassan Alsuhabi worked equally to this paper through writing, programming, and mathematics. All authors reviewed the results and approved the final version of the manuscript.

**Availability of Data and Materials:** The data that support the findings of this study are available from the corresponding author, upon reasonable request.

**Ethics Approval:** Not applicable.

**Conflicts of Interest:** The authors declare no conflicts of interest to report regarding the present study.

## References

1. Marshall AW, Olkin I. A new method for adding a parameter to a family of distributions with application to the exponential and Weibull families. Biometrika. 1997;84(3):641–52. doi:10.1093/biomet/84.3.641.
2. Mahdavi A, Kundu D. A new method for generating distributions with an application to exponential distribution. Communicat Statist-Theory Meth. 2017;46(13):6543–57. doi:10.1080/03610926.2015.1130839.
3. El-Morshedy M, Zubair A, Elsayed TE, Zahra AM, Eliwa Z, Iqbal. A new statistical approach for modeling the bladder cancer and leukemia patients data sets: case studies in the medical sector. Math Biosci Eng. 2022;10(19):10474–92. doi:10.3934/mbe.2022490.
4. Alshanbari HM, Ahmad Z, El-Bagoury AA, Odhah OH, Rao GS. A new modification of the weibull distribution: model, theory, and analyzing engineering data sets. Symmetry. 2024;16(5):611. doi:10.3390/sym16050611.
5. Ahmad Z, Mahmoudi E, Hamedani G. A family of loss distributions with an application to the vehicle insurance loss data. Pak J Stat Oper Res. 2019;15(3):731–44. doi:10.18187/pjsor.v15i3.2995.
6. ElSherpieny EA, Almetwally EM. The exponentiated generalized alpha power family of distribution: properties and applications. Pak J Stat Oper Res. 2022;18(2):349–67. doi:10.18187/pjsor.v18i2.3515.
7. Bashiru SO, Isa AM, Khalaf AA, Khaleel MA, Arum KC, Anioke CL. A hybrid cosine inverse lomax-G family of distributions with applications in medical and engineering data. Niger J Technol Dev. 2025;22(1):261–78. doi:10.4314/njtd.v22i1.2734.
8. Sadia N, Muhammad A, Kizito EA, Etaf A, Okechukwu JO. Group acceptance sampling plan based on truncated life tests for the Kumaraswamy Bell-Rayleigh distribution. Sci Afr. 2025;27(6):e02537. doi:10.1016/j.sciaf.2025.e02537.
9. Meraou MA, Al-Kandari N, Raqab MZ, Kundu D. Analysis of skewed data by using compound Poisson exponential distribution with applications to Insurance claims. J Stat Comput Simul. 2021;92(5):928–56. doi:10.1080/00949655.2021.1981324.
10. Meraou MA, Al-Kandari N, Raqab MZ. Univariate and bivariate compound models based on random sum of variates with application to the insurance losses data. J Stat Theory Pract. 2022;16(4):1–30. doi:10.1007/s42519-022-00282-8.
11. Meraou MA, Raqab MZ, Kundu D, Alqallaf F. Inference for compound truncated Poisson log-normal model with application to maximum precipitation data. Commun Stat Simul Comput. 2025;54(7):2796–817. doi:10.1080/03610918.2024.2328168.
12. Meraou MA, Raqab MZ, Almathkour FB. Analyzing insurance data with an alpha power transformed exponential poisson model. Ann Data Sci. 2024;12(3):991–1011. doi:10.1007/s40745-024-00554-z.
13. Almetwally EM, Meraou MA. Application of environmental data with new extension of nadarajah-haghighi distribution. Computat J Mathem Statist Sci. 2022;1(1):26–41. doi:10.21608/cjmss.2022.271186.
14. Alyami SA, Elbatal I, Alotaibi N, Almetwally EM, Elgarhy M. Modeling to factor productivity of the United Kingdom food chain: using a new lifetime-generated family of distributions. Sustainability. 2022;14(14):8942. doi:10.3390/su14148942.
15. Ahmad Z, Elgarhy M, Hamedani G, Butt NS. Odd generalized NH generated family of distributions with application to exponential model. Pak J Stat Oper Res. 2020;16(1):53–71. doi:10.18187/pjsor.v16i1.2295.

16. Aldahlan MA, Jamal F, Chesneau C, Elbatal I, Elgarhy M. Exponentiated power generalized Weibull power series family of distributions: properties, estimation and applications. PLoS One. 2020;15(3):e0230004. doi:10.1371/journal.pone.0230004.
17. Almarashi AM, Jamal F, Chesneau C, Elgarhy M. A new truncated muth generated family of distributions with applications. Complexity. 2021;2021(1):1211526. doi:10.1155/2021/1211526.
18. Al-Moisheer AS, Elbatal I, Almutiry W, Elgarhy M. Odd inverse power generalized Weibull generated family of distributions: properties and applications. Math Probl Eng. 2021;2021(1):5082192. doi:10.1155/2021/5082192.
19. Benchiha SA, Sapkota LP, Al Mutairi A, Kumar V, Khashab RH, Gemeay AM, et al. A new sine family of generalized distributions: statistical inference with applications. Math Comput Appl. 2023;28(4):83. doi:10.3390/mca28040083.
20. Orji GO, Etaga HO, Almetwally EM, Igbokwe CP, Aguwa OC, Obulezi OJ. A new odd reparameterized exponential transformed-X family of distributions with applications to public health data. Innovat Statist Probab. 2025;1(1):88–118. doi:10.64389/isp.2025.01107.
21. Saboor A, Jamal F, Shafq S, Mumtaz R. On the versatility of the unit logistic exponential distribution: capturingBathtub, upside-down bathtub, and monotonic hazard rates. Innovat Statist Probab. 2025;1(1):28–46. doi:10.64389/isp.2025.01102.
22. Sapkota LP, Kumar V, Tekle G, Alrweili H, Mustafa MS, Yusuf M. Fitting real data sets by a new version of gompertz distribution. Modern J Statist. 2025;1(1):25–48. doi:10.64389/mjs.2025.01109.
23. Eugene N, Lee C, Famoye F. Beta-normal distribution and its applications. Communicat Statist-Theory Meth. 2002;31(4):497–512. doi:10.1081/sta-120003130.
24. Moakofi T, Oluyede B, Chipepa F. Type II exponentiated half-logistic topp-leone marshall-olkin-g family of distributions with applications. Heliyon. 2021;7(12):e08590. doi:10.1016/j.heliyon.2021.e08590.
25. Azzalini A. A class of distributions which includes the normal ones. Scand J Stat. 1985;12:171–8. doi:10.2307/4615982.
26. Thomas B, Chacko V. Power generalized dus transformation in weibull and lomax distributions. Reliab Theory Applicat. 2023;1(72):368–84.
27. Hammad AT, Hafez EH, Shahzad U, Yıldırım E, Almetwally EM, Kibria BMG. New modified liu estimators to handle the multicollinearity in the beta regression model: simulation and applications. Modern J Statist. 2025;1(1):58–79. doi:10.64389/mjs.2025.01111.
28. Hassan AS, Alsadat N, Elgarhy M, Sapkota LP, Balogun OS, Gemeay AM. A novel asymmetric form of the power half-logistic distribution with statistical inference and real data analysis. Electr Res Arch. 2025;33(2):791–825. doi:10.3934/era.2025036.
29. Chinedu EQ, Chukwudum QC, Alsadat N, Obulezi OJ, Almetwally EM, Tolba AH. New lifetime distribution with applications to single acceptance sampling plan and scenarios of increasing hazard rates. Symmetry. 2023;15(10):1881. doi:10.3390/sym15101881.
30. Bashiru SO, Isa AM, Gemeay AM. Development and exploration of cosine rayleigh distribution. Develop Explorat Cosine Rayleigh Distrib. 2025;5(13):1–28. doi:10.28924/ada/stat.5.13.
31. Nwankwo MP, Najwan A, Anoop K, Mahmoud MB, Okechukwu JO. Group acceptance sampling plan based on truncated life tests for Type-I heavy-tailed Rayleigh distribution. Heliyon. 2024;10(19):e38150. doi:10.1016/j.heliyon.2024.e38150.
32. Alghamdi SM, Shrahili M, Hassan AS, Gemeay AM, Elbatal I, Elgarhy M. Statistical inference of the half logistic modified kies exponential model with modeling to engineering data. Symmetry. 2023;15(3):586. doi:10.3390/sym15030586.
33. Afify AZ, Gemeay AM, Alfaer NM, Cordeiro GM, Hafez EH. Power-modified Kies-exponential distribution: properties, classical and Bayesian inference with an application to engineering data. Entropy. 2022;24(7):883. doi:10.3390/e24070883.

34. Hassan AS, Mohamed RE, Kharazmi O, Nagy HF. A new four parameter extended exponential distribution with statistical properties and applications. Pak J Stat Oper Res. 2022;18(1):179–93. doi:10.18187/pjsor.v18i1.3872.
35. Hussein LK, Rasheed HA, Hussein IH. A class of exponential rayleigh distribution and new modified weighted exponential rayleigh distribution with statistical properties. Ibn AL-Haitham J Pure Appl Sci. 2023;36(2):390–406. doi:10.30526/36.2.3044.
36. Saeid A, Hanieh P, Chetan S, Showkat AL. Inference on adaptive progressive hybrid censored accelerated life test for Gompertz distribution and its evaluation for virus-containing micro droplets data. Alex Eng J. 2022;61(12):10071–84. doi:10.1016/j.aej.2022.02.061.
37. Abdelall YY, Hassan AS, Almetwally EM. A new extention of the odd inverse Weibull-G family of distributions: Bayesian and non-Bayesian estimation with engineering applications. Computat J Mathem Statist Sci. 2024;3(2):359–88. doi:10.21608/cjmss.2024.285399.1050.
38. AL-Dayian GR, EL-Helbawy A, Abd EL-Maksoud F. Bayesian and maximum likelihood estimation for mixture models of the new Topp-Leone-G Family. J Business Environ Sci. 2025;4(2):210–53. doi:10.21608/jcese.2024.330538.1084.
39. Sadiah MA, Aljeddani MA. Parameter estimation of a model using maximum likelihood function and Bayesian analysis through moment of order statistics. Alex Eng J. 2023;75(1):221–32. doi:10.1016/j.aej.2023.05.079.
40. Al-Babtain AA, Elbatal I, Almetwally EM. Bayesian and non-bayesian reliability estimation of stress-strength model for power-modified lindley distribution. Comput Intell Neurosci. 2022;2022(1):1154705. doi:10.1155/2022/1154705.
41. Marwan HA, Basim SO. Bayesian and classical inference of univariate maximum Harris extended Rayleigh model with applications. Alex Eng J. 2024;101(3):254–66. doi:10.1016/j.aej.2024.05.033.
42. Dutta S, Kayal S. Estimation and prediction for Burr type III distribution based on unified progressive hybrid censoring scheme. J Appl Stat. 2022;51(1):1–33. doi:10.1080/02664763.2022.2113865.
43. Dutta S, Kayal S. Estimation of parameters of the logistic exponential distribution under progressive type-I hybrid censored sample. Quality Technol Quantitat Manag. 2022;19(2):234–58. doi:10.1080/16843703.2022.2027601.
44. Dutta S, Kayal S. Bayesian and non-Bayesian inference of Weibull lifetime model based on partially observed competing risks data under unified hybrid censoring scheme. Qual Reliab Eng Int. 2022;2022(38):3867–91. doi:10.1002/qre.3180.
45. Dutta S, Alqifari HN, Almohaimeed A. Bayesian and non-bayesian inference for logistic-exponential distribution using improved adaptive type-II progressively censored data. PLoS One. 2024;19(5):e0298638. doi:10.1371/journal.pone.0298638.
46. Dutta S, Sultana F, Kayal S. Statistical inference for gumbel type-II distribution under simple step-stress life test using type-II censoring. Iran J Sci. 2023;47(1):155–73. doi:10.1007/s40995-022-01394-3.
47. Dutta S, Sultana F, Kayal S. Bayesian and non-Bayesian inference for a general family of distributions based on simple step-stress life test using TRV model under type II censoring. Seq Anal. 2023;42(4):349–70. doi:10.1080/07474946.2023.2224401.
48. Cheng R, Amin N. Estimating parameters in continuous univariate distributions with a shifted origin. J Royal Statist Soci Ser B (Methodological). 1983;45:394–403. doi:10.1111/j.2517-6161.1983.tb01268.x.
49. Jeffreys H. An invariant form for the prior probability in estimation problems. Proc Royal Soc London A: Mathem, Phys Eng Sci. 1946;186(1007):453–67. doi:10.1098/rspa.1946.0056.
50. Jeffreys H. Theory of probability. New York, NY, USA: Oxford University Press; 1961.
51. Chen MH, Shao QM. Monte Carlo estimation of Bayesian credible and HPD intervals. J Comput Graph Statist. 1999;8(1):69–92. doi:10.1080/10618600.1999.10474802.

52. Yusra AT, Bakr ME, Meraou MA, Anoop K, Yusuf M, Abd El-Raouf MM. A next generation probabilistic approach to analyze cancer patients data with inference and applications. Alex Eng J. 2025;114:147–72. doi:10.1016/j.aej.2024.11.079.
53. Badr A, Abdulaziz SA, Mohammad ZA, Maryam IH. Development of a new statistical distribution with insights into mathematical properties and applications in industrial data in KSA. AIMS Math. 2025;10(3):7463–88. doi:10.3934/math.2025343.
54. Arshad MZ, Iqbal MZ, Al Mutairi A. A comprehensive review of datasets for statistical research in probability and quality control. J Math Comput Sci. 2021;11(3):3663–728. doi:10.28919/jmcs/5692.
55. Eslam H, Maryam IH, Ramlah HA, Mohammed OM. Estimation of parameters for a new model: real data application and simulation. Alex Eng J. 2025;122:543–54. doi:10.1016/j.aej.2025.02.112.